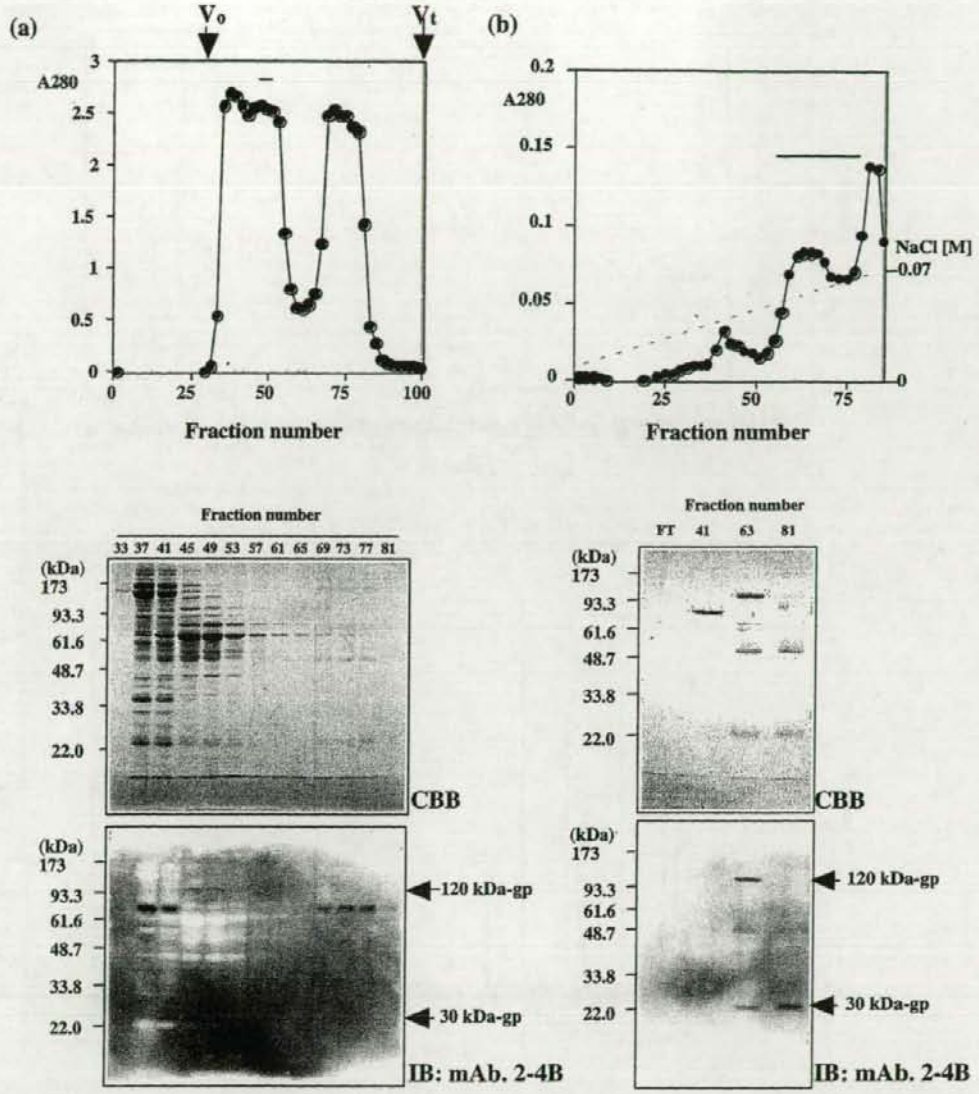

Fig. 2. Purification of the 30- and 120-kDa gp from normal mouse serum and MALDI-TOF MS analyses of their tryptic digest. (**a**) Sephacryl S-100 chromatography of 50% $(NH_4)_2SO_4$ precipitate of normal mouse serum (upper panel). Mouse serum was subjected to ammonium sulfate precipitation as described in *Materials and Methods*. The 50% $(NH_4)_2SO_4$ precipitate was applied to the column (1.3 × 75 cm) and eluted with 0.01 M NaCl in 10 mM Tris–HCl (pH 8.0). Elution was monitored by absorbance at 280 nm (V_0, void volume; V_t, total volume). Fractions were also monitored SDS–PAGE CBB staining (denoted as CBB, middle panel) and western blotting with mAb.2-4B (IB: 2-4B, lower panel). Aliquots (1 μL) of fractions 33–81 were loaded on a 10% polyacrylamide gel. Positions of the molecular mass markers are indicated on the left. The mAb.2-4B-immunoreactive proteins at 30- and 120-kDa gp-containing fractions (fractions 39–45) indicated by the bars were pooled. (**b**) DEAE-Toyopearl 650 M chromatography of the major 30- and 120-kDa gp-containing fractions in (**a**). The pooled fraction was applied to a DEAE-Toyopearl 650 M (Cl^- form; column size 1.2 × 17 cm) and eluted with a linear gradient of NaCl (0.01–0.07 M) in 0.01 M Tris–HCl (pH 8.0) (upper panel) as described in *Materials and Methods*. The NaCl concentration is shown by the dotted line. Elution profile was monitored by the absorbance at 280 nm. SDS–PAGE/CBB staining (denoted as CBB, middle panel) and western blotting with mAb.2-4B (IB: 2-4B) (lower panel) of fractions 41, 63, and 81 eluted from DEAE-Toyopearl 650 M chromatography were loaded on 10% polyacrylamide gel. Positions of the molecular mass markers are indicated on the left. The 30-kDa gp-containing fractions (fractions 56–79 at 0.050–0.065 M NaCl) were pooled as indicated by the bars. (**c**) MS spectrum (reflectron mode) of a tryptic digest of the 30-kDa gp. The 30-kDa gp band seen in (**b**) at fraction 81 was excised, digested in gel by trypsin, and analyzed by MALDI-TOF MS as described in *Materials and Methods*. (**d**) Sequence of the immunoglobulin light-chain κ-constant region (CAC20700). The putative sequences of observed peptides are summarized in Table I and are given in boldface type. (**e**) MS spectrum (reflectron mode) of a tryptic digest of the 120-kDa gp. The 120-kDa gp band observed in (**b**) at fraction 63 was excised, digested in gel by trypsin, and analyzed by MALDI-TOF MS as described in *Materials and Methods*. (**f**) Plasminogen sequence (AAA50168). The putative sequences of observed peptides are summarized in Table I and are underlined in boldface type.

(c)

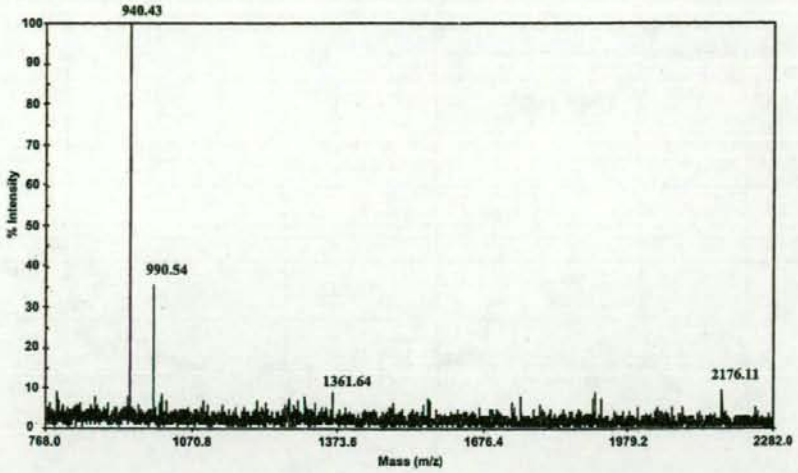

(d)

```
  1 ADAAPTVSIF PPSSEQLTSG GASVVCFLNN FYPKDINVK W KIDGSERQNG
  5 VLNSWTDQDS KDSTYSMSST LTLTKDEYER  HNSYTCEATH KTSTSPIVKS
101 FNRNEC
```

(e)

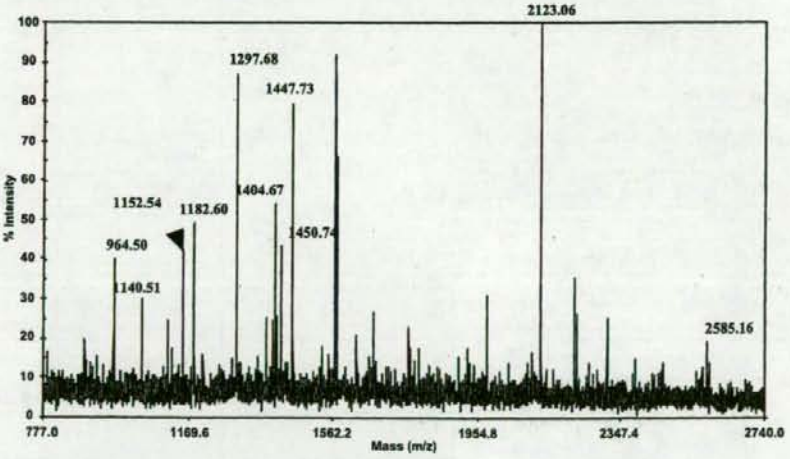

(f)

```
  1 MDHKEVILLF LLLLKPGQGD SLDGYISTQG ASLFSLTKK Q LAAGGVSDCL
 51 AKCEGETDFV CRSFQYHSKE QQCVIMAENS KTSSIIRMRD VILFEKRVYL
101 SECKTGIGNG YRGTMSRTKS GVACQKWGAT FPHVPNYSPS THPNEGLEEN
151 YCRNPDNDEQ GPWCYTTDPD KRYDYCNIPE CEEECMYCSG EKYEGKISKT
201 MSGLDCQAWD SQSPHAHGYI PAKFPSKNLK MNYCHNPDGE PRPWCFTTDP
251 TKRWEYCDIP RCTTPPPPPS PTYQCLKGRG ENYRGTVSVT VSGKTCQR WS
301 EQTPHRHNRT PENFPCKNLE ENYCRNPDGE TAPWCYTTDS QLRWEYCEIP
351 SCESSASPDQ SDSSVPPEEQ TPVVQECYQS DGQSYRGTSS TTITGKK CQS
401 WAAMFPHRHS KTPENFPDAG LEMNYCRNPD GDKGPWCYTT DPSVR WEYCN
451 LKRCSETGGS VVELPTVSQE PSGPSDSETD CMYGNGKDYR GK TAVTAAGT
501 PCQGWAAQEP HRHSIFTPQT NPRADLEKNY CRNPDGDVNG PWCYTTNPRK
551 LYDYCDIPLC ASASSFECGK PQVEPKKCPG RVVGGCVANP HSWPWQISLR
601 TRFTGQHFCG GTLIAPEWVL TAAHCLEKSS RPEFYKVILG AHEEYIRGLD
651 VQEISVAKLI LEPNNRDIAL LKLSRPATIT DKVIPACLPS PNYMVADRTI
701 CYITGWGETQ GTFGAGRLKE AQLPVIENK V CNRVEYLNNR VKSTELCAGQ
751 LAGGVDSCQG DSGGPLVCFE KDKYILQGVT SWGLGCARPN KPGVYVRVSR
801 FVDWIEREMR NN
```

Fig. 2. continued

Table I. Summary of the peptide sequences of peptide fragments obtained by MALDI-TOF MS analysis of the 30, 70, and 120-kDa gp purified from mouse serum

	Peptide sequence	MH^+ observed	Mr theoretical	Delta (Da)	Sequence coverage (%)
30-kDa gp	**WKIDGSER** (40–47)	990.54	989.49	0.04	32
	HNSYTCEATHK (81–91)	1361.64	1360.58	0.05	
	HNSYTCEATHKTSTSPIVK (81–99)	2175.11	2174.04	0.06	
	SFNRNEC (100–106)	940.43	939.39	0.03	
70-kDa gp	CTQGFMASKK (28–37)	1171.45	1170.55	–0.11	23
	GQYCYELDETAVRPGYPK (176–193)	2159.88	2159.00	–0.12	
	LIQDVWGIEGPIDAAFTR (194–211)	2000.91	2000.04	–0.14	
	TYLFK (218–222)	671.96	670.37	0.58	
	GSQYWR (223–228)	796.29	795.36	–0.08	
	FEDGVLDPGYPR (229–240)	1364.53	1363.64	–0.12	
	SSDGAREPQFISR (323–335)	1449.58	1448.70	–0.13	
	NWHGVPGKVDAAMAGR (336–351)	1665.69	1664.82	–0.13	
	IYVTGSLSHSAQAK (352–365)	1461.65	1460.76	–0.12	
120-kDa gp	QLAAGGVSDCLAKCEGETDFVCR (40–62)	2585.16	2584.17	–0.02	13
	WEYCDIPR (254–261)	1152.54	1151.51	0.03	
	WSEQTPHR (299–306)	1040.51	1039.48	0.02	
	WSEQTPHRHNR (299–309)	1447.73	1446.69	0.03	
	CQSWAAMFPHR (398–408)	1404.67	1403.62	0.04	
	WEYCNLKR (446–453)	1182.60	1181.57	0.03	
	TAVTAAGTPCQGWAAQEPHR (493–512)	2123.06	2122.00	0.05	
	HSIFTPQTNPR (513–523)	1297.68	1296.66	0.02	
	VCNRVEYLNNR (730–740)	1450.74	1449.71	0.02	
	FVDWIER (801–807)	964.50	963.48	0.01	

Boldface-type sequences were confirmed by MS/MS analyses.

MALDI-TOF MS analyses indicated that 30-, 70-, and 120-kDa gp mAb.2-4B-immunoreactive components were an Ig light chain, plasminogen, and vitronectin, respectively. To confirm these results, we purified these components from mouse serum by conventional methods and analyzed them for the presence of di/oligosialic acid using chemical analyses.

Affinity purification of the mouse Igs and demonstration of the presence of diSia

The partially purified 30-kDa gp obtained after DEAE-Toyopearl 650 M chromatography (Figure 2b) was applied to a Protein G-Sepharose column. After washing, Igs bound to the Protein G-Sepharose column were eluted with 50 mM diethylamine–HCl (pH 11.5). The purified IgGs were analyzed by western blotting using mAb.2-4B. The mAb.2-4B-positive 30-kDa gp(s) were bound to the Protein G-Sepharose column, which specifically traps the Fc region of IgG, and recovered in the diethylamine-eluted fraction (Figure 4a, elute). In SDS–PAGE/CBB analysis, the 30-kDa band moved up to the 170-kDa band under non-reducing conditions (data not shown). These findings together with the results obtained from MALDI-TOF MS (Figure 2c and d; Table I) confirmed that the 30-kDa gp is the IgG light chain.

To demonstrate the presence of diSia in the 30-kDa gp, we analyzed the purified IgG fraction by mild acid hydrolysis-fluorometric anion-exchange chromatography analysis and the fluorometric C_7/C_9 analysis. First, we analyzed the mild acid hydrolysate of the 30-kDa gp, which was labeled with a fluorescent reagent using anion-exchange chromatography. A Neu5Gc dimer was clearly observed, and higher oligomers were not observed (Figure 4b, middle panel). Then, we performed the fluorometric C_7/C_9 analysis. As summarized in Table II, C_9-Neu5Gc, which indicates the presence of internal sialic acid, was in the IgG fraction with a molar ratio of C_9-Neu5Gc to C_7-Neu5Gc of 0.09, suggesting that theoretically, ~9% of the sialic acid present on the molecule exists as diSia. These results indicate that the Ig light chain has diNeu5Gc residues. To determine the difference among the Ig classes or IgG subclasses, we analyzed a wide variety of monoclonal Igs. The light chains of IgG1, 2a, and 3, and other Ig classes, IgE and IgM, were immunostained with mAb.2-4B (Figure 4c, upper panel). To exclude the possibility of the non-specific binding of the secondary antibody, we used biotinylated mAb.2-4B and detected it with an avidin–biotin–peroxidase complex system. The same result obtained in Figure 4c was observed (data not shown). These data strongly indicate that the Ig light chains all contain the diNeu5Gc residues.

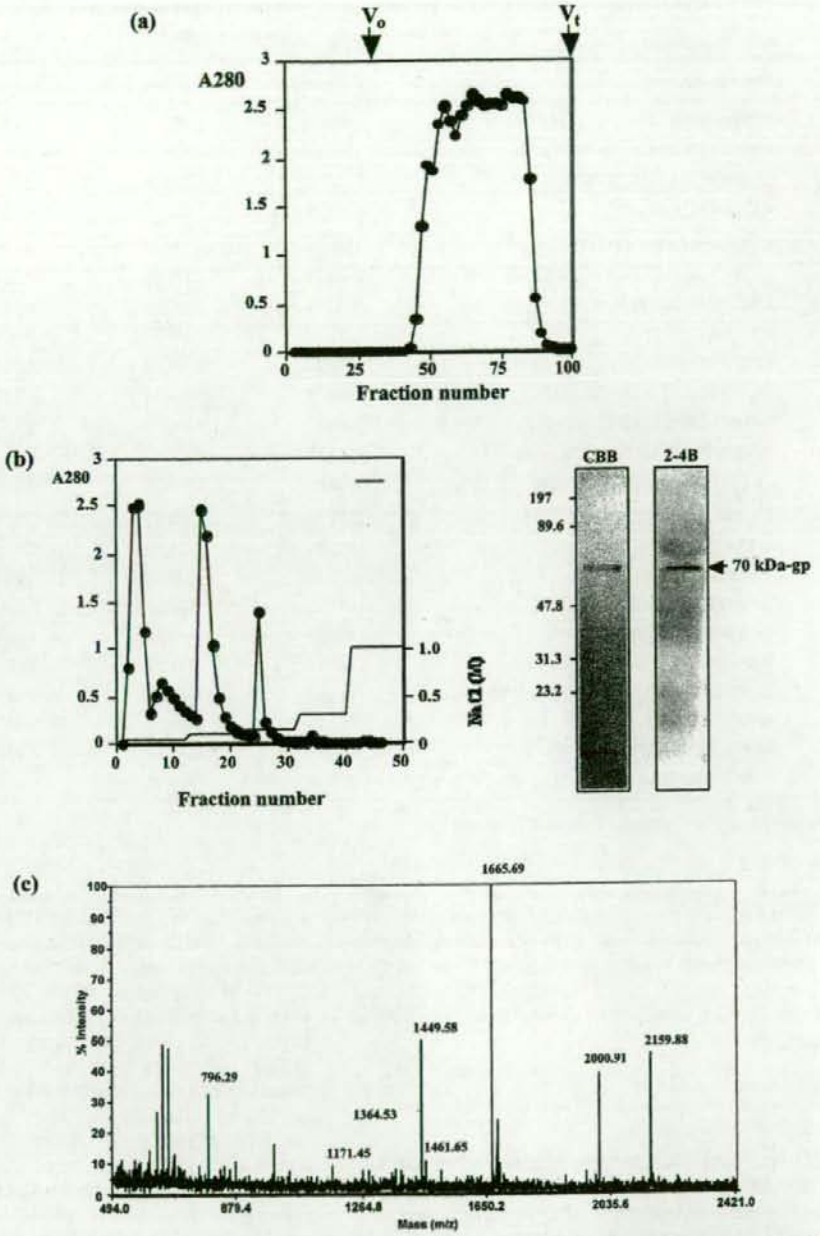

Fig. 3. Purification of the 70-kDa gp and MALDI-TOF MS analyses of its tryptic digest. (**a**) Sephacryl S-100 chromatography of 50% $(NH_4)_2SO_4$ p itate of inflamed mouse serum. Mouse serum was subjected to ammonium sulfate precipitation as described in *Materials and Methods*. The 50% $(NH_4)_2SO_4$ precipitate was applied to the column (1.3 × 75 cm) and eluted with 0.05 M NaCl in 50 mM Tris–HCl (pH 8.0). The elution profile was monitored by the absorbance at 280 nm and SDS–PAGE CBB and western blot using mAb. 2-4B (V_0, void volume; V_t, total volume). Major 70-kD gp-containing fractions (fractions 61–80) indicated by the bars were pooled. (**b**) DEAE-Toyopearl 650 M chromatography of the major 70-kDa gp-containing fraction in (**a**). The pooled fraction was applied to a DEAE-Toyopearl 650 M (Cl^- form; column size 1.0 × 24 cm) and eluted with discontinuous NaCl gradients in 0.05 M Tris–HCl (pH 8.0) as described in *Materials and Methods*. The NaCl concentration is shown by the line wit symbol. The elution profile was monitored by the absorbance at 280 nm (left panel). The 70-kDa gp-containing fractions (fractions 42–44 at 1.0 M were pooled as indicated by the bars, and the pooled fraction was examined by SDS–PAGE/CBB staining (denoted as CBB) and western blotting u mAb.2-4B (2-4B). (**c**) Positions of the molecular mass markers are indicated on the left. (**c**) MS spectrum (reflectron mode) of a tryptic digest of the 7 gp. The 70-kDa gp band observed in (**b**) was excised, digested in gel with trypsin, and analyzed by MALDI-TOF MS as described in *Materials and Methods*. (**d**) Vitronectin sequence (AAA40558). The putative sequences of observed peptides are summarized in Table I and are given in boldface t

(d)

```
  1 MAPLRPFFIL ALVAWVSLAD QESCKGRCTQ GFMASKKCQC DELCTYYQSC
 51 CADYMEQCKP QVTRGDVFTM PEDDYWSYDY VEEPKNNTNT GVQPENTSPP
101 GDLNPRTDGT LKPTAFLDPE EQPSTPAPKV EQQEEILRPD TTDQGTPEFP
151 EEELCSGKPF DAFTDLKNGS LFAFRGQYCY ELDETAVRPG YPKLIQDVWG
201 IEGPIDAAFT RINCQGKTYL FKGSQYWRFE DGVLDPGYPR NISEGFSGIP
251 DNVDAFALPA HRYSGRERVY FFKGKQYWEY EFQQQPSQEE CEGSSLSAVF
301 EHFALLQRDS WENIFELLFW GRSSDGAREP QFISRNWHGV PGKVDAAMAG
351 RIYVTGSLSH SAQAKKQKSK RRSRKRYRSR RGRGHRRSQS SNSRRSSRSI
401 WFSLFSSEES GLGTYNNYDY DMDWLVPATC EPIQVYFFSG DKYYRVNLRT
451 RRVDSVNPPY PRSIAQYWLG CPTSEK
```

Fig. 3. continued

Affinity purification of the mouse plasminogen and demonstration of the presence of di/oligoNeu5Gc

The 120-kDa gp that was specifically immunostained with mAb.2-4B was strongly indicated to be plasminogen by MALDI-TOF MS analyses (Figure 2e and Table I). A lysine-coupled column can be used to purify plasminogen (Edelberg *et al.*, 1990). Thus, normal mouse serum was applied to a lysine-coupled column. After washing, plasminogen was eluted with 300 mM phosphate buffer and 0.1 M 6-aminohexanoic acid in 100 mM phosphate buffer (pH 7.4). SDS–PAGE/CBB staining indicated that the plasminogen was highly purified (Figure 5, lanes 4 and 5), and western blot analysis of each fraction using mAb.2-4B demonstrated that the purified plasminogen contained the di/oligoNeu5Gc structure (Figure 5a, IB: 2-4B). To confirm the presence of diSia chemically, we analyzed plasminogen by mild acid hydrolysis-fluorometric anion-exchange chromatography. The diNeu5Gc structure was observed and higher oligomeric structures were not observed Figure 5b), although the amount of the diSia was not so large as that of IgGs. Then, we analyzed the plasminogen by the fluorometric C_7/C_9 analyses to confirm the presence of diSia (Table II). The ratio of C_9- to C_7-Neu5Gc residues suggested that 3% of the terminal end of the glycan chains were disialylated. The fact that the ratio was lower than that of IgG consists of the observation of the smaller diNeu5Gc peak derived from plasminogen than that from IgGs (Figure 4b). These findings clearly indicated that the mAb.2-4B-immunoreactive 120-kDa gp was plasminogen and that it contains the diNeu5Gc structure.

Affinity purification of mouse vitronectin and demonstration of the presence of diSia

Mouse vitronectin purified using a heparin column as described in *Materials and Methods* was immunostained with mAb.2-4B (data not shown). Based on the MALDI-TOF MS results shown in Figure 3 and Table I, we confirmed that the 70-kDa gp immunostained with mAb.2-4B was vitronectin. To demonstrate the diSia structure chemically, we analyzed the vitronectin by mild acid hydrolysis-fluorometric anion-exchange chromatography. The diNeu5Gc structure was clearly observed, and higher oligomeric structures were not observed (Figure 6a, middle panel). Furthermore, the fluorometric C_7/C_9 analysis of mouse vitronectin also showed the presence of C_9-Neu5Gc-DMB (Table II). The ratio of C_9- to C_7-Neu5Gc of 0.2 indicates that 20% of the terminal end of the sialyl glycan chain in mouse vitronectin is the diNeu5Gc structure. These immunochemical and chemical results clearly demonstrated that mouse vitronectin is modified by di/oligoNeu5Gc. The sialic acid detected in mouse vitronectin was exclusively Neu5Gc (Table II). To determine the difference between species, we also analyzed rat vitronectin. Purified rat vitronectin from serum was also immunostained with mAb.S2-566, which specifically recognizes the Neu5Acα2,8Neu5Acα2,3Gal structure (Figure 6b). The acid hydrolysis-anion exchange fluorometric high-performance liquid chromatography analyses showed that rat vitronectin has the diNeu5Ac structure, and higher oligoNeu5Ac structures were not observed (Figure 6c). These findings indicate that the diSia structure is present in rat vitronectin. Vitronectin is a multifunctional glycoprotein (McKeown-Longo and Panetti, 1996), and sialylation and *N*-glycosylation of vitronectin change markedly in partially hepatectomized rat (Uchibori-Iwaki *et al.*, 2000). Thus, we examined whether disialylation is altered by partial hepatectomy in rat. The purified vitronectin derived from the sera of normal, sham-operated, and partially hepatectomized rats were analyzed to determine the amount of protein by silver staining or the amount of diSia by immunostaining with mAb.S2-566 (Figure 6d), and the ratio of the amounts of diNeu5Ac to that of protein was quantified densitometrically (Figure 6e). Compared with normal rat vitronectin, the amount of diSia in sham-operated rat vitronectin decreased to 65% and that in partially hepatectomized rat vitronectin dramatically decreased to 30% (Figure 6e). These results demonstrate that the diSia structure in vitronectin changes following hepatectomy.

Discussion

In mouse serum, four components, a 30-, 32-, 70-, and 120-kDa gp, were immunoreactive with mAb.2-4B, which

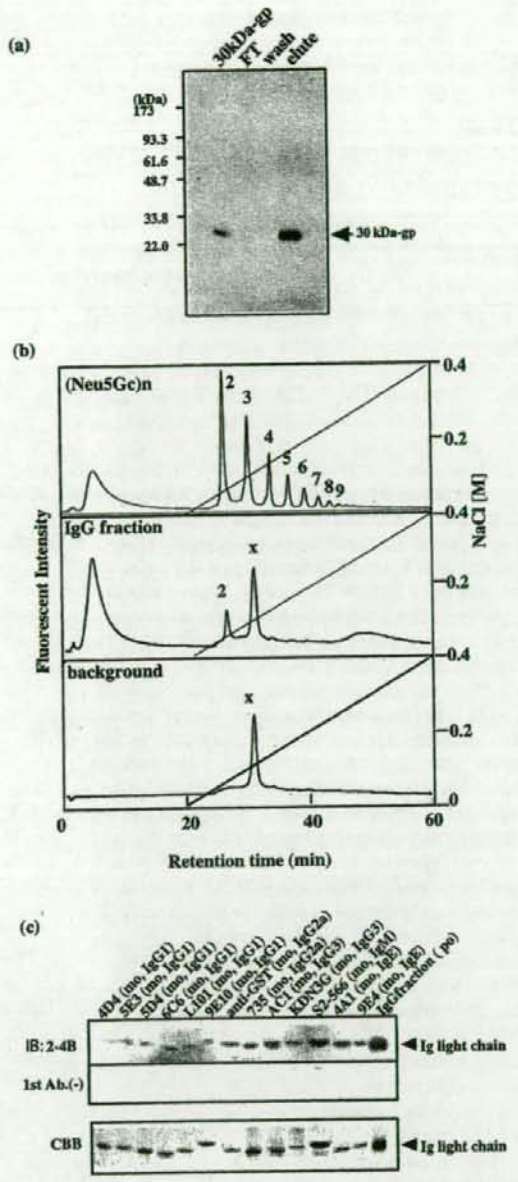

Fig. 4. Purified immunoglobulins (Igs) contained diNeu5Gc residues. (**a**) Protein G-Sepharose chromatography of the 30-kDa gp-containing fractions in Figure 2b. The fraction was applied to a Protein G-Sepharose column (0.7 mL) and eluted as described in *Materials and Methods*. The 30-kDa gp-containing fractions (1 μg as bovine serum albumin [BSA], 30-kDa gp), flow-through fraction (FT), wash fraction (Wash), and eluate fraction (Elute) were analyzed by western blotting using mAb.2-4B as a primary antibody. Positions of the molecular mass markers are indicated on the left. (**b**) Resource Q anion-exchange chromatography of di/oligo/polyNeu5Gc–DMB. Upper panel: α2→8-linked di/oligo/polyNeu5Gc derived from mild acid hydrolysates of polysialoglycoprotein [(Neu5Gc)*n*, 2 μg as Neu5Gc] labeled with DMB were applied to a Resource Q anion-exchange column (1 mL, Cl^- form). The column was eluted with 10 mM Tris–HCl (pH 8.0) with a gradient from 0–0.4 M NaCl as indicated by the thin line. The elution was monitored by a fluorescence detector (excitation 373 nm, emission 448 nm). The number at each peak represents the degree of polymerization (DP). Middle panel: IgG fraction, 30-kDa gp, (22 μg as BSA) was treated with 0.01 N trifluoroacetic acid at 50°C for 1 h, and released sialyloligomer was labeled with DMB. Labeled sialyloligomer was applied to a high-performance liquid chromatograph as described above. The peak labeled 'x' indicates an unidentified peak that was also detected in the background (bottom panel). (**c**) Western blot analyses of various Igs. Monoclonal Igs (0.3–5 μg as BSA/lane) were subjected to SDS–PAGE/CBB staining (denoted as CBB) and western blotting with mAb.2-4B (IB: 2-4B) or without primary antibody [1st antibody (-)]. mo, monoclonal; po, polyclonal. IgG fraction obtained from mouse serum was also analyzed (IgG fraction).

specifically recognizes the di/oligoNeu5Gc structure (Yasukawa *et al.*, 2005). Our ultimate goal is to determine the function of disialylation in these molecules, and as a first step, we identified the protein components of these molecules in this study. Recently, we identified the 32-kDa gp as carbonic anhydrase II and demonstrated that it is an acute-phase inflammatory protein (Yasukawa Z *et al.*, in preparation). We purified three other mAb.2-4B-immunoreactive components from mouse serum using several chromatographic steps. MALDI-TOF MS analyses demonstrated that the 30-, 70-, and 120-kDa gp were an Ig light chain, vitronectin, and plasminogen, respectively.

Ig light chains were purified from mouse serum, and this glycoprotein was confirmed by three methods to have diSia. One method was immunoblotting using the anti-di/oligoNeu5Gc antibody, mAb.2-4B. The other two were chemical methods. We observed diNeu5Gc residues by anion-exchange chromatography after 1,2-diamino-4,5-methylenedioxybenzene (DMB) labeling of mild acid hydrolysates of Ig (Figure 4b). The fluorometric C_7/C_9 analyses of purified Ig also showed that ~9% of the terminal sialylglycan chains were disialylated based on the ratio of C_9 to C_7 of Neu5Gc (Table II). The amount of Neu5Ac was 3% that of Neu5Gc, and Neu5Ac was also present as diSia according to the ratio of C_9- to C_7-Neu5Ac (Table II). The presence of sialic acid residues, especially in the mouse light-chain Ig fraction, but not in the heavy-chain fraction, and the findings that IgM and IgE as well as IgG light chains were modified with diSia (Figure 4c) suggest that disialylation is important for the biologic processes of Igs. It is widely reported that IgG contains 2.3 *N*-linked biantennary oligosaccharide chains per molecule in mice (Mizuochi *et al.*, 1987; Raju *et al.*, 2000), and two of these represent the conserved glycosylation sites at Asn-297 in each of the two heavy-chain C_H2 domains of the Fc portion, and the remainder is found in the hypervariable regions of the Fab section with the frequency and position dependent on the chance occurrence of the *N*-glycosylation consensus sequence (Asn-Xaa-Thr/Ser). (Parekh *et al.*, 1985; Mizuochi *et al.*, 1987). Variations in the *N*-glycosylation of IgG molecules at one conserved site, Asn-297, in the Fc region can directly modulate Fc-receptor recognition and effector functions (Dwek *et al.*, 1995; Lund *et al.*, 1995, 1996; Wright and Morrison, 1998). *O*-glycosylation in the Fc portion has also been detected in two mouse monoclonal IgG2a antibodies in dot blot experiments using lectins (Coco-Martin *et al.*, 1992). Approximately 40% of the heavy chains of the mouse IgG2b antibodies are *O*-glycosylated at

Table II. Fluorescent C_7/ C_9 analyses of the 30-, 70-, and 120-kDa gp

	Neu5Gc			Neu5Ac		
Sia species	C_9[a] (mol/mol)	C_7 (mol/mol)	C_9/C_7	C_9[a] (mol/mol)	C_7 (mol/mol)	C_9/C_7
30-kDa gp	0.011	0.13	0.09	0.0023	0.0022	1.0
70-kDa gp	0.38	2.2	0.2	Trace	Trace	
120-kDa gp	0.010	0.31	0.03	0.0036	0.017	0.2

Neu5Gc, *N*-glycolylneuraminic acid.
[a]C_9 indicates internal sialic acid via the α2,8-linkage.

Thr-221A in the hinge region, and *O*-glycosylation might be involved in protease resistance (Kim *et al.*, 1994). *O*-glycosylation of the IgG1 light chain is reported on a chimeric antibody (cMu-9–1) (Krishnan *et al.*, 1999). In the present study, we first found that mouse Ig light chains contained diNeu5Gc residues. Because of the ubiquitous presence of diSia in Ig light chains, it might be useful to examine the presence of diSia in Bence-Jones protein, which is secreted into urine due to an imbalance in the amounts of heavy and light chains in plasma cells (Bradwell *et al.*, 2003; Miller *et al.*, 2004). It is important to examine the presence of diSia on such Igs derived during disease states.

The 120-kDa gp was identified as plasminogen, and this glycoprotein also contained diSia in mouse serum. In human serum, plasminogen is present in two major glycoforms, plasminogen 1, which possesses an *N*-linked high mannose-type carbohydrate chain at Asp-289 and an *O*-linked carbohydrate chain at Thr-345, and plasminogen 2, which contains an *O*-linked glycan at Thr-345 (Hayes and Castellino, 1979a; Davidson and Castellino, 1991; Pirie-Shepherd *et al.*, 1997). The *O*-linked carbohydrate chain at Thr-345 is Neu5Acα2→3Galβ1→3GalNAc (Hayes and Castellino, 1979b; Davidson and Castellino, 1991). Plasminogen 2 can be separated into at least six glycoforms according to the Neu5Ac content by isoelectric focusing electrophoresis (Siefring and Castellino, 1974; Gonzalez-Gronow *et al.*, 1990). The Neu5Ac content of plasminogen 2 varies from 1.3 to 13.7 mol/mol protein (Pirie-Shepherd *et al.*, 1995), suggesting the presence of a sialyloligo/polymer. Each glycoform isolated by two dimensional-PAGE of plasminogen 2 displays markedly different kinetic behaviors when activated with tissue-plasminogen activator, urinary-type plasminogen activator, and streptokinase (Pirie-Shepherd *et al.*, 1995, 1996). In this study, mouse plasminogen was shown to have diSia, and this glycoform of plasminogen might regulate tissue plasminogen activator, urinary-type plasminogen activator, and streptokinase.

Vitronectin in mouse and rat also has diSia (Figure 6a and c). Vitronectin is a multifunctional adhesive glycoprotein that originates mainly in hepatocytes and circulates in the blood stream at high concentrations (0.2 mg/mL in humans) (Uchibori-Iwaki *et al.*, 2000). Vitronectin regulates the blood systems related to protease cascades, such as cell lysis, by complement, coagulation, and fibrinolysis (Tomasini and Mosher, 1990; Preissner, 1991). Vitronectin is also found in the extracellular matrix of most tissues and is considered to have a role in cell adhesion, cellular motility, and matrix remodeling. Tissue vitronectin is considered to be present as an active multimeric form, and interactions with various matrix ligands, such as various types of integrins on the cell surfaces, Type-1 plasminogen activator inhibitor, and urokinase receptors, to regulate pericellular proteolysis (McKeown-Longo and Panetti, 1996; Seiffert, 1997; Preissner and Seiffert, 1998), are responsible for these functions. Vitronectin can also bind to various types of collagen through its conformational transition from the native inactive form to an active form (Gebb *et al.*, 1986; Ishikawa-Sakurai and Hayashi, 1993; Izumi *et al.*, 1998). Vitronectins from various animals (human, horse, porcine, bovine, rabbit, and chicken) react with several lectins (*Canavalia ensiformis*, *Triticum vulgare*, *Allomyrina dichotoma*, *Ulex europeaeus*, *Lens culinaris* agglutinin, and *Phaseolus vulgaris* leukoagglutinin) (Kitagaki-Ogawa *et al.*, 1990). In addition, the *N*-linked oligosaccharide structures of porcine (Yoneda *et al.*, 1993) and human plasma vitronectins (Ogawa *et al.*, 1995) have been elucidated. Carbohydrate composition and lectin reactivity indicate that *N*-glycosylation and sialylation of vitronectin change markedly after partial hepatectomy. Vitronectins from partially hepatectomized rats 24 h after surgery exhibit markedly enhanced binding to Type-I collagen, and equal enhancement of collagen binding was caused by desialylation of vitronectin with sialidase treatment (Uchibori-Iwaki *et al.*, 2000). These results suggest that modulation of the biologic activity of vitronectin is achieved through altered glycosylation. In this study, we demonstrated that vitronectin was modified by diSia. In particular, the amounts of disialylation of vitronectin derived from hepatectomized rat dramatically decreased compared with that of normal rat (Figure 6e), suggesting that diSia residues regulate the function of vitronectin in sera to regenerate the liver. The fact that diSia in sham-operated rat vitronectin decreased compared to that of normal rat suggests that the inflammation caused by tissue injury reduces the disialylation state of vitronectin, although inflammation caused by turpentine oil, which produces the interleukin-1 and interleukin-6 cascade (Won *et al.*, 1993), does not change the disialylation state in serum.

Based on the fact that diSia is present in plasminogen, vitronectin, and α_2 macroglobulin (Kitajima *et al.*, 1999), it might have an important role in the regulation of protease activity. It is noteworthy that some proteases have a basic cluster and a key basic amino acid near active sites that regulates protease activity (Cheng *et al.*, 1986; Rezaie and Yang, 2003). Owing to the negative charge of diSia, it might bind to these basic amino acids to inhibit function. As plasminogen and vitronectin have major roles in fibrinolytic activity in

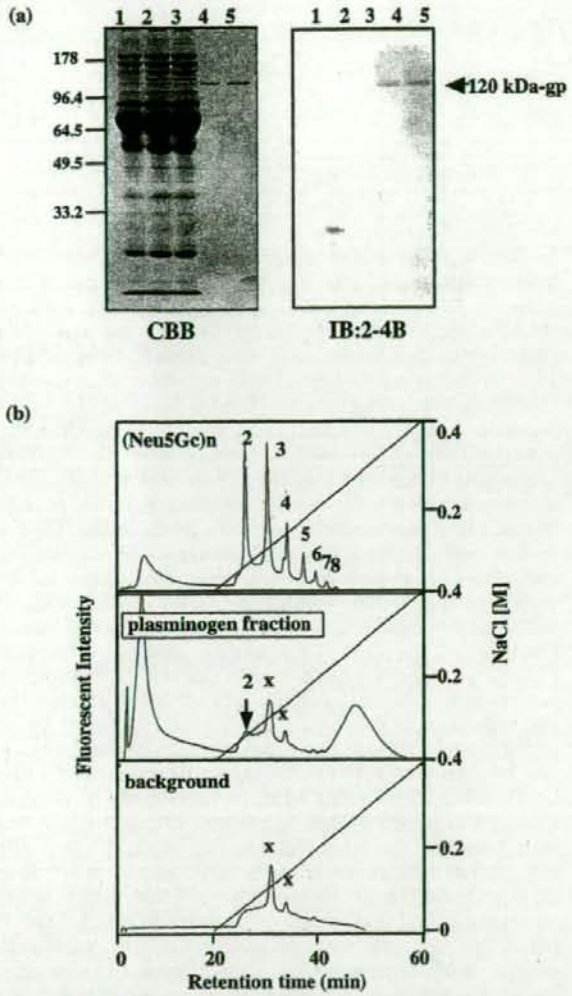

Fig. 5. Affinity-purified plasminogen contained diNeu5Gc residues. (**a**) SDS–PAGE/CBB and western blotting using mAb.2-4B (IB: 2-4B) of the fractions eluted from the lysine-Sepharose. Mouse serum were applied to a lysine-Sepharose and eluted as described in *Materials and Methods*. Mouse serum (15 μg, lane 1), flow-through from non-coupled Sepharose 4B (15 μg, lane 2), flow-through from lysine-Sepharose (15 μg, lane 3), 300 mM phosphate buffer (pH 7.4) eluate (0.2 μg, lane 4), and 0.1 M 6-aminohexanoic acid in 100 mM phosphate buffer (pH 7.4) eluate (0.2 μg, lane 5) were analyzed. Positions of the molecular mass markers are indicated on the left. (**b**) Resource Q anion-exchange chromatography of di/oligo/polyNeu5Gc–DMB. *Upper panel*: α2→8-linked di/oligo/polyNeu5Gc derived from mild acid hydrolysates of polysialoglycoprotein [(Neu5Gc)*n*, 2 μg as Neu5Gc]. The conditions were described in *Materials and Methods* and in Figure 4b. Middle panel: 120-kDa gp of plasminogen fraction (5.4 μg as bovine serum albumin) was treated with 0.01 N trifluoroacetic acid at 50°C for 1 h, and released sialyloligomer was labeled with DMB. Labeled sialyloligomer was applied to the high-performance liquid chromatography analysis as described above. The peak labeled 'x' indicates an unidentified peak that is also detected in background (bottom panel).

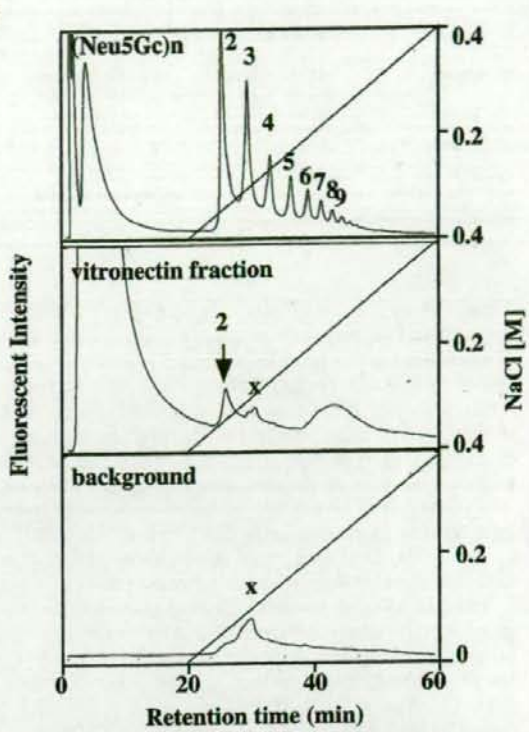

Fig. 6. Mouse and rat vitronectin contained diNeu5Gc and diNeu5Ac, respectively, and the diNeu5Ac residues on rat vitronectin decreased after partial hepatectomy. (**a**) Resource Q anion-exchange chromatography of di/oligo/polyNeu5Gc–DMB. Upper panel: α2→8-linked di/oligo/polyNeu5Gc derived from mild acid hydrolysates of polysialoglycoprotein [(Neu5Gc)*n*, 2 μg as Neu5Gc] labeled with DMB were applied to a Resource Q anion-exchange column (1 mL, Cl^- form). The conditions are described in *Materials and Methods* and in Figure 4b. Middle panel: 70-kDa gp of vitronectin fraction (21 μg as BSA) was treated with 0.01 N trifluoroacetic acid at 50°C for 1 h, and released sialyloligomer was labeled with DMB. Labeled sialyloligomer was applied to a high-performance liquid chromatograph as described above. The peak labeled 'x' indicates an unidentified peak that was also detected in the background (bottom panel). (**b**) SDS–PAGE/silver staining (silver) and western blot analysis using mAb.S2-566 (IB: S2-566 [specific to Neu5Acα2→8Neu5Acα2→3Gal structure]) of vitronectin from normal rat serum. Positions of molecular mass markers are indicated on the left. (**c**) Resource Q anion-exchange chromatography of di/oligo/polyNeu5Ac–DMB. Upper panel: α2→8-linked di/oligo/polyNeu5Ac derived from mild acid hydrolysates of colominic acid [(Neu5Ac)*n*, 10 μg as Neu5Ac] labeled with DMB were applied to a Resource Q anion-exchange column (1 mL, Cl^- form). The conditions are described in the *Materials and Methods* and in Figure 4b. Middle panel: Purified rat vitronectin (3.2 μg as BSA) was treated with 0.01 N trifluoroacetic acid at 50°C for 1 h, and released sialyloligomer was labeled with DMB. Labeled sialyloligomer was applied to the high-performance liquid chromatograph as described above. The peak labeled 'x' indicates an unidentified peak that was also detected in the background (bottom panel). (**d**) SDS–PAGE/silver staining (silver) and western blotting using mAb.S2-566 of vitronectin derived from non-operated rat (NO-VN), sham-operated rat (SH-VN), and partially hepatectomized rat (PH-VN). Vitronectin (0.1 μg/lane) was analyzed. (**e**) The ratio of the amount of diNeu5Ac on vitronectin to the protein amount of vitronectin decreased after partial hepatectomy. The amount of diNeu5Ac and the protein of vitronectin were densitometrically quantified, and the relative ratio of disialic acid to the protein amount of the vitronectin derived from normal serum was set equal to 1.0. The bars indicate standard deviation ($n = 3$).

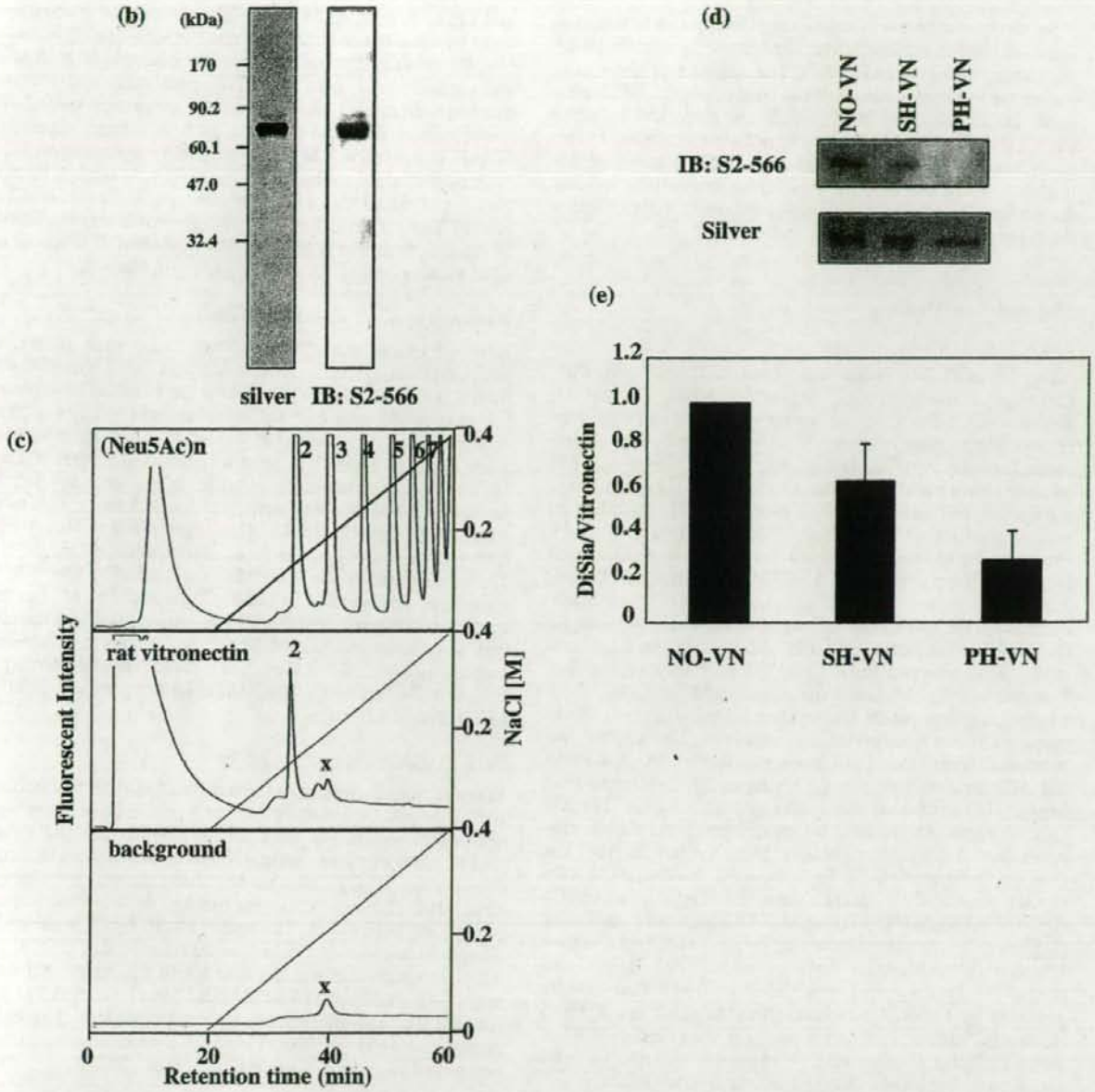

Fig. 6. continued

sera, diSia might regulate fibrinolytic activity via inhibition of proteases in sera.

It has been shown that two sialyltransferases, ST8Sia III and VI, are responsible for the synthesis of diSia structures. ST8Sia III catalyzes the synthesis of disialic and oligosialic acids on glycolipids, glycoproteins, and oligosaccharides (Yoshida *et al.*, 1995; Angata *et al.*, 2000), whereas ST8Sia VI acts on *O*-glycans as well as oligosaccharides (Takashima *et al.*, 2002; Teintenier-Lelievre *et al.*, 2005). ST8Sia III is strongly expressed in fetal brain and testis (Tsuji, 1999). We reported that ST8Sia III was moderately up-regulated during neural differentiation of Neuro2A cells (Sato *et al.*, 2002) and during adipogenesis of 3T3-L1 cells (Sato *et al.*, 2001). The expression of ST8Sia VI is ubiquitous in various cells and tissues (Takashima *et al.*, 2002). In mouse liver, we previously demonstrated that ST8Sia III and VI were constantly expressed before and after inflammation (Yasukawa *et al.*, 2005). Therefore, these sialyltransferases might synthesize the diSia structure on vitronectin, plasminogen, and the light chain of antibodies.

In serum, natural antibodies are present, and sometimes, these antibodies are involved in diseases such as neuropathy (Kornberg and Pestronk, 1995). The antigens of these antibodies are sometimes considered to be gangliosides (O'Hanlon *et al.*, 2002; Schwerer, 2002), which are mimicked by some bacterial lipopolysaccharides or lipooligosaccharides. In this study, we demonstrated the presence of diSia in serum glycoproteins. Thus, diSia might be an immunogen that induces the production of anti-ganglioside antibodies that are sometimes present in sera as natural antibodies.

Materials and Methods

Materials

Silver Stain II Kit Wako was obtained from Wako Pure Chemical (Osaka, Japan). Sephacryl S-100, Protein G-Sepharose, CNBr-activated Sepharose resins, and enhanced chemiluminescence reagents were purchased from Amersham Biosciences (Piscataway, NJ). DEAE-Toyopearl 650 M resins were purchased from Tosoh (Tokyo, Japan). Polyvinylidene difluoride (PVDF) membrane (Immobilon P) was a product obtained from Millipore (Bedford, MA). Prestained molecular weight markers were purchased from Bio-Rad (Hercules, CA), Daiichi Pure Chemicals (Tokyo, Japan), or Sigma Chemical (St. Louis, MO). Peroxidase-conjugated rat anti-mouse IgG was purchased from American Qualex (San Clemente, CA). Peroxidase-conjugated rat anti-mouse IgM was purchased from Zymed Laboratories, (San Francisco, CA). Mouse monoclonal IgM antibody 2-4B, which recognizes Neu5Gcα2→(8Neu5Gcα2→)$_{n-1}$, $n \geq 2$, was prepared as described previously (Sato *et al.*, 1998). DMB was purchased from Dojindo (Kumamoto, Japan). Male, 8-week-old ddY mice were obtained from Japan SLC, (Hamamatsu, Japan). Turpentine oil was kindly provided by Dr. Hiroaki Oda (Nagoya University, Nagoya, Japan). Avidin–biotin–peroxidase complex was obtained from Vectastain ABC Kit (Vector Laboratories, Burlingame, CA). mAbs., mAb.4D4 (IgG1), mAb.5D4 (IgG1), mAb.5E9 (IgG1), mAb.6C6 (IgG1), mAb.L101 (IgG1), mAb.4A1 (IgE), and mAb.9E4 (IgE) were kindly provided by Dr. Tsukasa Matsuda (Nagoya University). mAb.AC1 (IgG3), mAb.9E10 (IgG1) and mAb.735 (IgG2a), and mAb.S2-566 (IgM) were kindly provided by Dr. Keiko Nohara (National Institute of Environmental Studies, Tsukuba, Japan), Dr. Rita Gerady-Schahn (Medizinische Hochschule, Hannover, Germany), and Dr. Koichi Furukawa (Nagoya University), respectively.

Experimental inflammation

Turpentine oil was injected subcutaneously into ddY mice to induce inflammation, and sera were prepared as described previously (Yasukawa *et al.*, 2005).

Purification of the 30- and 120-kDa gp from mouse serum

Normal mouse sera (9.3 mL) was mixed with 9.3 mL of saturated $(NH_4)_2SO_4$ (final concentration, 50%), stirred at 4°C for 1 h and centrifuged at 10,000 × *g* for 10 min. The pellet was dissolved in 10 mM Tris–HCl (pH 8.0) containing 0.1 M NaCl and applied to Sephacryl S-100 chromatography (1.3 × 75 cm, 100 mL, equilibrated with 10 mM Tris–HCl [pH 8.0] containing 0.1 M NaCl). The elution profile was monitored by absorbance at 280 nm and by SDS–PAGE followed by CBB staining. Glycoproteins were separated by SDS–PAGE and electroblotted onto a PVDF membrane and immunostained with mAb.2-4B. The fractions containing mAb.2-4B-immunoreactive 30 and 120-kDa gp were pooled, applied to DEAE-Toyopearl 650 M chromatography (column size: 1.2 × 1.7 cm, buffer: 10 mM Tris–HCl [pH 8.0] containing 10 mM NaCl), and eluted with a linear gradient of 10–70 mM NaCl in 10 mM Tris–HCl (pH 8.0). The elution profile was monitored by the absorbance at 280 nm and by SDS–PAGE followed by CBB staining and western blotting using mAb.2-4B.

Purification of the 70-kDa gp from mouse serum

Inflamed mouse sera (20 mL) was mixed with 20 mL of saturated $(NH_4)_2SO_4$ (final concentration, 50%), stirred at 4°C for 3 h, and centrifuged at 10,000 × *g* for 15 min. The supernatant was mixed with 26.6 mL of saturated $(NH_4)_2SO_4$ (final concentration, 70%), stirred at 4°C for 12 h, and centrifuged at 10,000 × *g* for 15 min. The pellet was dissolved in 50 mM Tris–HCl (pH 8.0) containing 50 mM NaCl and applied to Sephacryl S-100 chromatography (1.3 × 80.5 cm, equilibrated with 50 mM Tris–HCl [pH 8.0] containing 50 mM NaCl). Elution was monitored as described *Purification of the 30-and 120-kDa mouse serum*. The fractions containing the 70-kDa gp were pooled, applied to DEAE-Toyopearl 650 M chromatography (column size: 1.0 × 24 cm, buffer: 50 mM Tris–HCl [pH 8.0] containing 50 mM NaCl), and eluted in a step-wise manner with 0.05, 0.1, 0.15, 0.3, and 1.0 M NaCl containing 50 mM Tris–HCl (pH 8.0). The 70-kDa gp was purified in the 1.0 M NaCl-eluted fraction.

SDS–PAGE and western blotting

Samples were dissolved in Laemmli buffer with 5% mercaptoethanol and boiled at 100°C for 3 min. The samples were electrophoresed in 7 or 10% polyacrylamide gels and visualized by CBB or silver staining. Glycoproteins were electroblotted onto PVDF membranes using a semidry blotting apparatus. The membrane was blocked with 10 mM sodium phosphate buffer (pH 7.2) and 0.15 M NaCl with 0.05% Tween-20 containing 1% bovine serum albumin at 25°C for 1 h. The membrane was incubated with a primary antibody, mAb.2-4B (0.50 μg/mL) or mAb.S2-566 (1.0 μg/mL) at 4°C for 16 h. The secondary antibody was peroxidase-conjugated anti-mouse IgM (1/5000 diluted). Color development was performed as described earlier (Sato *et al.*, 2000).

Two-dimensional gel electrophoresis

Two-dimensional PAGE was performed with a PROTEAN IEF Cell (Bio-Rad) using 7-cm pH 3–10 ReadyStrip IPG Strip (Bio-Rad). Protein samples were resuspended in rehydration buffer (9.8 M urea, 4% CHAPS, and 100 mM dithiothreitol [DTT]) at a ratio of 1 : 3. Isoelectric focusing was performed at 250 V for 15 min, 250–4000 V linear ramp for 2 h, and 4000 V for 5 h at 20°C. After the gel strips were equilibrated for 10 min in 6 M urea, 2% SDS, 0.375 M Tris–HCl (pH 8.8), 20% glycerol, and 130 mM DTT, and then re-equilibrated for 10 min in the same buffer containing 135 mM iodoacetamide in place of DTT. The proteins were separated by SDS–PAGE.

In-gel digestion and MALDI-TOF MS

In-gel trypsin digestion of CBB-stained bands and MALDI-TOF MS analyses were performed as described (Yasukawa *et al.*, 2005).

Affinity purification of IgG

The 30-kDa gp-enriched fraction was applied to the Protein G-Sepharose column. The column was washed with 10 mM Tris–HCl (pH 8.0) containing 0.15 M NaCl and eluted with 50 mM diethylamine–HCl (pH 11.5). The eluted solution was quickly neutralized with 1 M Tris–HCl (pH 8.0).

Affinity purification of plasminogen

L-lysine monohydrochloride (15 mg; Wako Pure Chemical) was coupled with 5 mL of CNBr-activated Sepharose 4B, according to the manufacturer's instructions. Normal mouse sera (6.2 mL) were applied to the non-coupled Sepharose 4B (Amersham Biosciences, Piscataway, NJ), which was equilibrated with 100 mM phosphate buffer (PB; pH 7.4). The pass-through fraction was re-applied to a lysine-coupled Sepharose column, which was equilibrated with 100 mM PB (pH 7.4). The column was washed with 100 mM PB (pH 7.4), 300 mM PB (pH 7.4), and eluted with 100 mM PB (pH 7.4) containing 0.1 M 6-aminohexanoic acid (Sigma).

Affinity purification of vitronectin

Vitronectin was purified from mouse sera, according to the previously described method (Yatohgo *et al.*, 1988; Kitagaki-Ogawa *et al.*, 1990). In brief, serum was passed through a heparin-Sepharose column and supplemented with a final concentration of 8 M urea. The serum was charged again on a heparin-Sepharose affinity column in the presence of 8 M urea. Vitronectin was specifically bound to the column and eluted with 0.5 M NaCl in the presence of 8 M urea.

Fluorescent C_7/C_9 analysis and mild acid hydrolysis–DMB derivatization followed by anion-exchange chromatography

Fluorescent C_7/C_9 analyses were performed as described earlier (Sato, Inoue, *et al.*, 1998). Mild acid hydrolysis–DMB derivatization followed by anion-exchange chromatography was conducted as described previously (Sato *et al.*, 1999).

Hepatectomy of rat and purification of vitronectin from serum

Vitronectins from non-operated, sham-operated, and partially hepatectomized rat plasma were purified as described previously (Uchibori-Iwaki *et al.*, 2000).

Acknowledgements

We thank Dr. Tsukasa Matsuda (Nagoya University) for his valuable discussion and providing us monoclonal antibodies. This research was supported in part by Grants-in-Aid for Scientific Research (C) (15570096) (to K.K.), CREST of Japan Science and Technology Corporation (to K.K.), the 21st Century COE Program (to K.K.), Young Scientists (B) (18770083) (to C.S.), Priority Areas and the Japan Society (17046006) (to C.S.) for the Promotion of Science Research Fellows (16005841) (to Z.Y.) from the Ministry of Education, Science, Sports and Culture, and Mizutani Foundation (to C.S.).

Conflict of interest statement

None declared.

Abbreviations

BSA, bovine serum albumin; diSia, disialic acid; DMB, 1,2-diamino-4,5-methylenedioxybenzene; DTT, dithiothreitol; Neu5Ac, *N*-acetylneuraminic acid; Neu5Gc, *N*-glycolylneuraminic acid; PB, phosphate buffer; PVDF, polyvinylidene difluoride; SDS–PAGE, sodium dodecyl sulfate–polyacrylamide gel electrophoresis.

References

Angata, T. and Varki, A. (2002) Chemical diversity in the sialic acids and related alpha-keto acids: an evolutionary perspective. *Chem. Rev.*, **102**, 439–469.

Angata, K., Suzuki, M., McAuliffe, J., Ding, Y., Hindsgaul, O., and Fukuda, M. (2000) Differential biosynthesis of polysialic acid on neural cell adhesion molecule (NCAM) and oligosaccharide acceptors by three distinct alpha 2,8-sialyltransferases, ST8Sia IV (PST), ST8Sia II (STX), and ST8Sia III. *J. Biol. Chem.*, **275**, 18594–18601.

Ashwell, G. and Morell, A.G. (1974) The role of surface carbohydrates in the hepatic recognition and transport of circulating glycoproteins. *Adv. Enzymol. Relat. Areas Mol. Biol.*, **41**, 99–128.

Bradwell, A.R., Carr-Smith, H.D., Mead, G.P., Harvey, T.C., and Drayson, M.T. (2003) Serum test for assessment of patients with Bence Jones myeloma. *Lancet*, **361**, 489–491.

Browning, L.M., Krebs, J.D., and Jebb, S.A. (2004) Discrimination ratio analysis of inflammatory markers: implications for the study of inflammation in chronic disease. *Metabolism*, **53**, 899–903.

Cheng, H.C., Kemp, B.E., Pearson, R.B., Smith, A.J., Misconi, L., Van Patten, S.M., and Walsh, D.A. (1986) A potent synthetic peptide inhibitor of the cAMP-dependent protein kinase. *J. Biol. Chem.*, **261**, 989–992.

Coco-Martin, J.M., Brunink, F., van der Velden-de Groot, T.A.M., and Beuvery, E.C. (1992) Analysis of glycoforms present in two mouse IgG2a monoclonal antibody preparations. *J. Immunol. Methods*, **155**, 241–248.

Davidson, J.D. and Castellino, J.F. (1991) Structures of the asparagine-289-linked oligosaccharides assembled on recombinant human plasminogen expressed in a Mamestra brassicae cell line (IZD-MBO503). *Biochemistry*, **30**, 6689–6696.

Drickamer, K. (1991) Clearing up glycoprotein hormones. *Cell*, **67**, 1029–1032.

Dwek, R.A., Lellouch, A.C., and Wormald, M.R. (1995) Glycobiology: the function of sugar in the IgG molecule. *J. Anat.*, **187**, 279–292.

Edelberg, J.M., Enghild, J.J., Pizzo, S.V., and Gonzalez-Gronow, M. (1990) Neonatal plasminogen displays altered cell surface binding and activation kinetics. *J. Clin. Invest.*, **86**, 107–112.

Gebb, C., Hayman, E.G., Engvall, E., and Ruoslahti, E. (1986) Interaction of vitronectin with collagen. *J. Biol. Chem.*, **261**, 16698–16703.

Gonzalez-Gronow, M., Grenett, E.H., Fuller, M.G., and Pizzo, V.S. (1990) The role of carbohydrate in the function of human plasminogen. *Biochim. Biophys. Acta*, **1039**, 269–276.

Hayes, M.L. and Castellino, J.F. (1979a) Carbohydrate of the human plasminogen variants. *J. Biol. Chem.*, **254**, 8768–8771.

Hayes, M.L. and Castellino, F.J. (1979b) Carbohydrate of the human plasminogen variants. *J. Biol. Chem.*, **254**, 8777–8780.

Ishikawa-Sakurai, M. and Hayashi, M. (1993) Two collagen N-binding domains of vitronectin. *Cell Struct. Funct.*, **18**, 253–259.

Izumi, M., Shimo-Oka, T., Morishita, N., Li, I., and Hayashi, M. (1998) Identification of the collagen-binding domain of vitronectin using monoclonal antibodies. *Cell Struct. Funct.*, **13**, 217–225.

Kim, H., Yamaguchi, Y., Masuda, K., Matsunaga, C., Yamamoto, K., Irimura, T., Takahashi, N., Kato, K., and Arata, Y. (1994) *O*-glycosylation in hinge region of mouse immunoglobulin G2b. *J. Biol. Chem.*, **269**, 12345–12350.

Kitagaki-Ogawa, H., Yatohgo, T., Izumi, M., Hayashi, M., Kashiwagi, H., Matsumoto, I., and Seno, N. (1990) Diversities in animal vitronectins. *Biochim. Biophys. Acta*, **1033**, 49–56.

Kitajima, K., Sato, C., Honda, N., Matsuda, T., Hara-Yokoyama, M., Close, B.E., and Colley, K.J. (1999) Occurrence of alpha2,8-linked oligosialic acid residues in mammalian glycoproteins. In Inoue, Y., Lee, Y.C., and Troy, F.A. (eds), *Sialobiology and Other Novel Form of Glycosylation, A Monograph*. Gakushin Syuppan, Osaka, Japan, pp. 69–76.

Kornberg, A.J. and Pestronk, A. (1995) Chronic motor neuropathies: diagnosis, therapy, and pathogenesis. *Ann. Neurol.*, **37**, S43–S50.

Krishnan, I.S., Hansen, H.J., Gold, D.V., Goldenberg, D.M., and Leung, S.O. (1999) Co-secretion of two distinct kappa light chains by the mu-9 hybridoma. *Hybridoma*, **18**, 325–333.

Lund, J., Takahashi, N., Pound, D.J., Goodall, M., Nakagawa, H., and Jefferis, R. (1995) Oligosaccharide–protein interactions in IgG can modulate recognition by Fc gamma receptors. *FASEB J.*, **9**, 115–119.

Lund, J., Takahashi, N., Pound, J.D., Goodall, M., and Jefferis, R. (1996) Multiple interactions of IgG with its core oligosaccharide can modulate recognition by complement and human Fc gamma receptor I and influence the synthesis of its oligosaccharide chains. *J. Immunol.*, **157**, 4963–4969.

McKeown-Longo, P.J. and Panetti, T.S. (1996) Structure and function of vitronectin. *Trends Glycosci. Glycotechnol.*, **8**, 327–340.

Miller, I., Teinfalt, M., Leschnik, M., Wait, R., and Gemeiner, M. (2004) Nonreducing two-dimensional gel electrophoresis for the detection of Bence Jones proteins in serum and urine. *Proteomics*, **4**, 257–260.

Mizuochi, T., Hamako, J., and Titani, K. (1987) Structures of the sugar chains of mouse immunoglobulin G. *Arch. Biochem. Biophys.*, **257**, 387–394.

Nagai, Y. and Iwamori, M. (1995) Cellular biology of gangliosides. In Rosenberg, A. (ed.), *Biology of the Sialic Acids*. Plenum Press, New York, pp. 197–241.

Ogawa, H., Yoneda, A., Seno, N., Hayashi, M., Ishizuka, I., Hase, S., and Matsumoto, I. (1995) Structures of the N-linked oligosaccharides on human plasma vitronectin. *Eur. J. Biochem.*, **230**, 994–1000.

O'Hanlon, G.M., Bullens, R.W., Plomp, J.J., and Willison, H.J. (2002) Complex gangliosides as autoantibody targets at the neuromuscular junction in Miller Fisher syndrome. *Neurochem. Res.*, **27**, 697–709.

Parekh, B.R., Dwek, A.R., Sutton, J.B., Fernandes, L.D., Leung, A., Stanworth, D., Rademacher, W.T., Mizuochi, T., Taniguchi, T., Matsuta, K., and others (1985) Association of rheumatoid arthritis and primary osteoarthritis with changes in the glycosylation pattern of total serum IgG. *Nature*, **316**, 452–457.

Petersen, H.H., Nielsen, J.P., and Heegaard, P.M.H. (2004) Application of acute phase protein measurements in veterinary clinical chemistry. *Vet. Res.*, **35**, 163–187.

Pirie-Shepherd, S.R., Jett, E.A., Andon, N.L., and Pizzo, S.V. (1995) Sialic acid content of plasminogen 2 glycoforms as a regulator of fibrinolytic activity. *J. Biol. Chem.*, **270**, 5877–5881.

Pirie-Shepherd, S.R., Serrano, R.L., Andon, N.L., Gonzalez-Gronow, M., and Pizzo, S.V. (1996) The role of carbohydrate in the activation of plasminogen 2 glycoforms by streptokinase. *Fibrinolysis*, **10**, 49–53.

Pirie-Shepherd, S.R., Stevens, R.D., Andon, N.L., Enghild, J.J., and Pizzo, S.V. (1997) Evidence for a novel *O*-linked sialylated trisaccharide on Ser-248 of human plasminogen 2. *J. Biol. Chem.*, **272**, 7408–7411.

Preissner, T.K. (1991) The role of sialic acid in the determination of distinct properties of the isozymes of rabbit plasminogen. *Annu. Rev. Cell Biol.*, **7**, 275–310.

Preissner, T.K. and Seiffert, D. (1998) Role of vitronectin and its receptors in haemostasis and vascular remodeling. *Thromb. Res.*, **89**, 1–21.

Raju, T.S., Briggs, J.B., Borge, S.M., and Jones, A.J. (2000) Species-specific variation in glycosylation of IgG: evidence for the species-specific sialylation and branch-specific galactosylation and importance for engineering recombinant glycoprotein therapeutics. *Glycobiology*, **10**, 477–486.

Rezaie, A.R. and Yang, L. (2003) Thrombomodulin allosterically modulates the activity of the anticoagulant thrombin. *Proc. Natl. Acad. Sci. U. S. A.*, **100**, 12051–12056.

Sato, C. (2004) Chain length diversity of sialic acids and its biological significance. *Trends Glycosci. Glycotechnol.*, **16**, 331–344.

Sato, C., Fukuoka, H., Ohta, K., Matsuda, T., Koshino, R., Kobayashi, K., Troy, F.A., 2nd, and Kitajima, K. (2000) Frequent occurrence of pre-existing α2→8-linked disialic and oligosialic acids with chain lengths up to 7 Sia residues in mammalian brain glycoproteins. *J. Biol. Chem.*, **275**, 15422–15431.

Sato, C., Inoue, S., Matsuda, T., and Kitajima, K. (1998) Development of a highly sensitive chemical method for detecting α2→8-linked oligo/polysialic acid residues in glycoproteins blotted on the membrane. *Anal. Biochem.*, **261**, 191–197.

Sato, C., Inoue, S., Matsuda, T., and Kitajima, K. (1999) Fluorescent-assisted detection of oligosialyl units in glycoconjugates. *Anal. Biochem.*, **266**, 102–109.

Sato, C., Kitajima, K., Inoue, S., and Inoue, Y. (1998) Identification of oligo-*N*-glycolylneuraminic acid residues in mammal-derived glycoproteins by a newly developed immunochemical reagent and biochemical methods. *J. Biol. Chem.*, **273**, 2575–2582.

Sato, C., Matsuda, T., and Kitajima, K. (2002) Neural differentiation-dependent expression of the disialic acid epitope on CD166 and its involvement in neural formation in neuro 2A cells. *J. Biol. Chem.*, 277, 45299–45305.

Sato, C., Yasukawa, Z., Honda, N., Matsuda, T., and Kitajima, K. (2001) Identification and adipocyte differentiation-dependent expression of the unique disialic acid residues in an adipose tissue specific glycoprotein, adipo Q. *J. Biol. Chem.*, **276**, 28849–28856.

Schauer, R. (2004) Sialic acids: fascinating sugars in higher animals and man. *Zoology*, **107**, 49–64.

Schwerer, B. (2002) Antibodies against gangliosides. *Microbes Infect.*, **4**, 373–384.

Seiffert, D. (1997) Constitutive and regulated expression of vitronectin. *Histol. Histopathol.*, **12**, 787–797.

Sharon, N. and Lis, H. (1997) Glycoproteins: structure and function. In Gabius, H.-J. and Gabius, S. (eds), *Glycosciences: Status and Perspectives*. Chapman & Hall, Weinheim, Germany, pp. 133–189.

Siefring, G.E. Jr. and Castellino, F.J. (1974) The role of sialic acid in the determination of distinct properties of the isozymes of rabbit plasminogen. *J. Biol. Chem.*, **249**, 7742–7746.

Sillanaukee, P., Ponnio, M., and Jaaskelainen, I.P. (1999) Occurrence of sialic acids in healthy humans and different disorders. *Eur. J. Clin. Invest.*, **29**, 413–425.

Takashima, S., Ishida, H.K., Inazu, T., Ando, T., Ishida, H., Kiso, M., Tsuji. S., and Tsujimoto, M. (2002) Molecular cloning and expression of a sixth type of α2,8-sialyltransferase (ST8Sia VI) that sialylates *O*-glycans. *J. Biol. Chem.*, **277**, 24030–24038.

Teintenier-Lelievre, M., Julien, S., Juliant, S., Guerardel, Y., Duonor-Cerutti, M., Delannoy, P., and Harduin-Lepers, A. (2005) Molecular cloning and expression of a human hST8Sia VI (α2,8-sialyltransferase) responsible for the synthesis of the diSia motif on *O*-glycosylproteins. *Biochem. J.*, **392**, 665–674.

Tomasini, B.R. and Mosher, D.F. (1990) Vitronectin. In Coller, B.S. (ed.), *Progress in Hemostasis and Thrombosis*. Saunders, Philadelphia/Sydney, pp. 269–305.

Tsuji, S. (1999) Molecular cloning and characterization of mouse sialyltransferases. In Inoue, Y., Lee, Y.C., and Troy, F.A. (eds), *Sialobiology and Other Novel Form of Glycosylation, A Monograph*. Gakushin Syuppan, Osaka, Japan, pp. 145–154.

Uchibori-Iwaki, H., Yoneda, A., Oda-Tamai, S., Kato, S., Akamatsu, N., Otsuka, M., Murase, K., Kojima, K., Suzuki, R., Maeya, Y., and others. (2000) The changes in glycosylation after partial hepatectomy enhance collagen binding of vitronectin in plasma. *Glycobiology*, **10**, 865–874.

Won, K.-A., Campos, S.P., and Baumann, H. (1993) Experimental systems for studying hepatic acute phase response. In Mackiewicz, A., Kushner, I., and Baumann, H. (eds), *Acute Phase Proteins*. CRC Press, Boca Raton, F.L., pp. 255–271.

Wright, A. and Morrison, S.L. (1998) Effect of C2-associated carbohydrate structure on Ig effector function: studies with chimeric mouse-human IgG1 antibodies in glycosylation mutants of Chinese hamster ovary cells. *J. Immunol.*, **160**, 3393–3402.

Yasukawa, Z., Sato, C., and Kitajima, K. (2005) Inflammation-dependent changes in α2,3-, α2,6-, and α2,8-sialic acid glycotopes on serum glycoproteins in mice. *Glycobiology*, **15**, 827–837.

Yatohgo, T., Izumi, M., Kashiwagi, H., and Hayashi, M. (1988) Novel purification of vitronectin from human plasma by heparin affinity chromatography. *Cell Struct. Funct.*, **13**, 281–292.

Yoneda, A., Ogawa, H., Matsumoto, I., Ishizuka, I., Hase, S., and Seno, N. (1993) Structures of the N-linked oligosaccharides on porcine plasma vitronectin. *Eur. J. Biochem.*, **218**, 797–806.

Yoshida, Y., Kojima, N., Kurosawa, N., Hamamoto, T., and Tsuji, S. (1995) Molecular cloning of Sia α2,3Galβ1,4GlcNAc α2,8-sialyltransferase from mouse brain. *J. Biol. Chem.*, **270**, 14628–14633.

Glycobiology vol. 16 no. 10 pp. 891–901, 2006
doi:10.1093/glycob/cwl016
Advance Access publication on June 13, 2006

Novel carbohydrate-binding activity of bovine liver β-glucuronidase toward lactose/*N*-acetyllactosamine sequences

Hiroko Matsushita-Oikawa[1,3], Mayumi Komatsu[1,3], Naoko Iida-Tanaka[4], Hiromi Sakagami[3], Tetsuko Kanamori[3], Isamu Matsumoto[3], Nobuko Seno[3], and Haruko Ogawa[2,3,5]

[3]Course of Advanced Biosciences, Graduate School of Humanities and Sciences, Tokyo, Japan; [4]Department of Food Science, Otsuma University, Tokyo, Japan; and [5]The Glycoscience Institute, Ochanomizu University, Tokyo, Japan

Received on August 31, 2005; revised on May 18, 2006; accepted on June 11, 2006

β-Glucuronidase is a lysosomal enzyme that plays an essential role in normal turnover of glycosaminoglycans and remodeling of the extracellular matrix components in both physiological and inflammatory states. The regulation mechanisms of enzyme activity and protein targeting of β-glucuronidase have implications for the development of a variety of therapeutics. In this study, the effectiveness of various carbohydrate-immobilized adsorbents for the isolation of bovine liver β-glucuronidase (BLG) from other glycosidases was tested. β-Glucuronidase and contaminating glycosidases in commercial BLG preparations bound to and were coeluted from adsorbents immobilized with the substrate or an inhibitor of β-glucuronidase, whereas β-glucuronidase was found to bind exclusively with lactamyl–Sepharose among the adsorbents tested and to be effectively separated from other enzymes. Binding and elution studies demonstrated that the interaction of β-glucuronidase with lactamyl–Sepharose is pH dependent and carbohydrate specific. BLG was purified to homogeneity by lactamyl affinity chromatography and subsequent anion-exchange high-performance liquid chromatography (HPLC). Lactose was found to activate β-glucuronidase noncompetitively, indicating that the lactose-binding site is different from the substrate-binding site. Binding studies with biotinyl glycoproteins, lipids, and synthetic sugar probes revealed that β-glucuronidase binds to *N*-acetyllactosamine/lactose-containing glycoconjugates at neutral pH. The results indicated the presence of *N*-acetyllactosamine/lactose-binding activity in BLG and provided an effective purification method utilizing the novel carbohydrate binding activity. The biological significance of the carbohydrate-specific interaction of β-glucuronidase, which is different from the substrate recognition, is discussed.

Key words: affinity purification/glycoprobe/lactose and *N*-acetyllactosamine-binding/lysosomal enzyme/zymography/β-glucuronidase

Introduction

β-Glucuronidase is an exoglycosidase that cleaves β-glucuronic acid linkages from the nonreducing termini of glycosaminoglycans such as chondroitin sulfate, heparan sulfate, and hyaluronic acid. It is present in animals, plants, and bacteria as an essential enzyme for the normal degradation and turnover of components of the extracellular matrix (Paigen, 1989). In animals, β-glucuronidase is widely distributed in tissues, and high activity is detected in spleen, liver, and kidney; it also serves in the incorporation of β-glucuronides of steroid hormones into tissues. Bovine liver β-glucuronidase (BLG) [EC 3. 2. 1. 31] has been reported to be a homotetramer of 290 kDa (Himeno *et al.*, 1974) and to have *N*-linked oligosaccharides with mannose 6-phosphate (Kaplan and Achord, 1977) (Natwicz *et al.*, 1982), which is a targeting signal to lysosomes recognized by specific Golgi receptors to segregate BLG into transport vesicles via a glycan-specific sorting mechanism (Kornfeld, 1987).

β-Glucuronidase from bovine liver is commercially available from several manufacturers. However, most β-glucuronidase preparations are contaminated with many other proteins including several glycosidases, such as *N*-acetyl-β-hexosaminidases and β-galactosidase. It is difficult to separate β-glucuronidase from the lysosomal protein mixtures, and multiple purification steps have been required for β-glucuronidase preparation, that is, a combination of several methods using serial fractionations with ammonium sulfate, ethanol, and organic solvents, gel filtration chromatography, ion-exchange chromatography, and isoelectric chromatofocusing (Himeno *et al.*, 1974; Ho, 1991). In this study, we were trying to isolate BLG from commercial preparations, and while searching for a suitable affinity adsorbent among those immobilized with various carbohydrates including its inhibitor and substrates, we unexpectedly discovered that BLG has binding activity toward lactamyl–Sepharose. Interaction of BLG with glycoconjugates and the effect of carbohydrates on the enzyme activity provide new insights into the biological functions of the carbohydrate binding of β-glucuronidase.

Materials and methods

Materials

Commercial BLG was purchased from Worthington Biochemical Co. (Lakewood, NJ) in most experiments as a crude enzyme preparation and from P-L Biochemicals (present Pharmacia P-L Biochemicals Inc., Milwaukee, WI) or from Sigma-Aldrich Co. (St. Louis, MO) for comparison. p-Nitrophenyl-β-D-glucuronide, 5-bromo-4-chloro-3-indolyl

[1]These two authors contributed equally to this article.
[2]To whom correspondence should be addressed;
e-mail: hogawa@cc.ocha.ac.jp

(X-) β-D-glucuronide, ceramide (bovine brain), and galactosylceramide (bovine spinal cord) were purchased from Wako Pure Chemicals (Osaka, Japan). *p*-Nitrophenyl-β-D-galactoside was purchased from Nakalai Tesque Inc. (Kyoto, Japan). *p*-Nitrophenyl-β-D-galactoside, transferrin, fetuin, ovalbumin, bovine submaxillary gland mucin (BSM), bovine lactosylceramide, human spleen glucosylceramide, galactosylceramide, ceramide, bovine brain sulfatide, and streptavidin-biotinylated horseradish peroxidase complex (ABC-HRP) were purchased from Sigma-Aldrich Co. Saccharo-1,4-lactone and β-galactosidase (from jack bean) were purchased from Seikagaku Kogyo (Tokyo, Japan). All biotinylated glycoprotein probes and their deglycosylated derivatives were prepared in our laboratory. Biotinylation was performed using EZ-link™sulfo-NHS-biotin (Pierce, Rockford, IL) according to the instruction manual. Asialoglycoproteins, asialo-agalactoglycoproteins, and ahexosamino-asialoagalactoglycoproteins were prepared from biotinylated glycoproteins by sequential glycosidase treatments with *Vibrio cholerae* neuraminidase (Roche Diagnostics, Basel, Switzerland) (0.1 units/mg glycoprotein) in 20 mM sodium acetate-buffered saline (pH 5.5), jack bean β-galactosidase (Seikagaku Kogyo) (0.14 units/mg glycoprotein) in 50 mM sodium citrate buffer (pH 3.5) and then β-N-acetylhexosaminidase (1.43 units/mg glycoprotein) in 50 mM sodium citrate buffer (pH 5.0), each at 37°C overnight. Biotinyl polymer (BP) sugar probes were purchased from GlycoTech Co. (Gaithersburg, MD).

Preparation of affinity adsorbents

Affinity adsorbents containing various carbohydrates as ligands were prepared using Sepharose 4B gel (Pharmacia, Uppsala, Sweden) in our laboratory. Lactose, maltose, melibiose, glucose, galactose, *N*-acetylchitotriose and *N*-acetylchondrosine were immobilized to amino Sepharose by reductive amination (Matsumoto *et al.*, 1981) Saccharo-1,4-lactone was immobilized to amino Sepharose with the aid of *N*-ethyl-*N'*-(3-dimethyl aminopropyl)-carbodiimide hydrochloride (Harris *et al.*, 1973). *p*-Aminophenyl β-glucuronide was immobilized to formyl Sepharose by reductive amination (Ito *et al.*, 1985). The immobilized carbohydrate concentrations of the adsorbents (μmol per g wet gel) were 45 for saccharo-1,4-lactone-, 35 for *N*-acetylchondrosine-, and 30–35 for other neutral saccharides coupled by reductive amination; lactamyl, maltamyl, melibiamyl, glucamyl, galactamyl and *N*-acetylchitotriamyl Sepharose. Those of *p*-aminophenylglucuronide- and *N*-acetylchitotriose-Sepharose were not determined.

Preparation of 1-deoxy-4-O-β-D-galactopyranosyl-1-([2-hydroxyethyl]amino)-D-glucitol and analysis by nuclear magnetic resonance spectroscopy

1-Deoxy-4-*o*-β-D-galactopyranosyl-1-([2-hydroxyethyl]amino)-D-glucitol (GHAG) was prepared by coupling 2-aminoethanol (366 μL) with lactose (0.3 M solution, 7.5 mL) by reductive amination with the pH adjusted to 7.5 with acetic acid. After preincubation for 2 h at 40°C, 300 mg of $NaBH_3CN$ was added and incubated for 2 h at 90°C; progress of the coupling reaction was confirmed by TLC (Holmes and O'Brien, 1979). The reaction mixture was diluted to 100 mL with water and applied to a charcoal column (2 × 35 cm), followed by washing with water and elution with a 0–20% gradient of ethanol. For determination of the structure, ^{1}H- and ^{13}C-nuclear magnetic resonance (NMR) spectra were obtained by using an ECA-800 spectrometer (JEOL, Tokyo) with a probe temperature of 60°C. The purified product was dried over P_2O_5 under vacuum and dissolved in $(CD_3)_2SO$ (Me_2SO-d_6). Chemical shifts were referenced to tetramethylsilane. Spectral parameters of double quantum-filtered correlated spectroscopy (DQF-COSY), total correlated spectroscopy (TOCSY), heteronuclear multiple-quantum coherence (HMQC), and heteronuclear multiple-bond correlation (HMBC) spectra were as described previously (Iida-Tanaka *et al.*, 2002).

Binding of β-glucuronidase with various carbohydrate-immobilized Sepharose gels

Interactions between various adsorbents and BLG were studied by affinity chromatography on a small column (0.75 × 4.5 cm, Vt=2 mL). Commercial BLG (6 mg from Pharmacia P-L Biochemicals) was dissolved in 1 mL of 2 mM sodium acetate buffer–5 mM NaCl (pH 7.0) (buffer A) and applied to each column. The column was washed with buffer A and then sequentially eluted with 5 mM sodium acetate buffer–5 mM NaCl (pH 5.0) (buffer B), 10 mM sodium acetate buffer–5 mM NaCl (pH 5.0) (buffer C), 25 mM sodium acetate buffer–5 mM NaCl (pH 5.0) (buffer D), 50 mM sodium acetate buffer–5 mM NaCl (pH 5.0) (buffer E), 50 mM sodium acetate buffer–50 mM NaCl (pH 5.0) (buffer F), and 0.2 M sodium acetate buffer–0.2 M NaCl (pH 5.0) (buffer G). The eluted fractions (2 mL/fraction) were measured for enzyme activities, and proteins were detected by absorbance at 280 nm.

Binding and elution of BLG to lactamyl Sepharose

Lactamyl Sepharose 4B (0.1 g) and 1 mg of BLG (from Worthington) were incubated at 4°C for 4 h in a 1.5-mL tube with 0.3 mL of various buffers: 2 mM sodium acetate buffer (pH 5–6), ammonium acetate (pH 6), or Tris–HCl (pH 6–9), each containing 5 mM NaCl. After centrifugation at 900 *g* for 5 min, the supernatant was removed, and the gel was washed three times with the same buffer; then the bound proteins were eluted with buffer G for 4 h at 4°C, and the enzyme activity of the eluted fraction was measured. To study the elution conditions from lactamyl Sepharose gel, we incubated BLG with lactamyl Sepharose gel in 0.2 mL of 2 mM sodium acetate buffer–5 mM NaCl (pH 6.0) (buffer A'). After centrifugation, the supernatant was removed, the gel was washed three times with buffer A', then incubated in each solution for 4 h at 4°C, and the enzyme activity of the eluted fraction was measured.

Purification of BLG on a lactamyl–Sepharose column and anion-exchange high-performance liquid chromatography

For large-scale purification, the binding of BLG to lactamyl–Sepharose was performed by a batch-wise method to improve the binding capacity. BLG (Worthington or Sigma, 15 mg) was mixed with 13 mL of lactamyl-Sepharose 4B in buffer A' and incubated for 5 h at 4°C with

gentle shaking, and then, the gel was poured into a column (1.5 × 8 cm). After extensive washing with buffer A′, BLG was successively eluted with buffer C, 25 mM sodium acetate buffer–25 mM NaCl (pH 5.0) (buffer E′), and buffer G. Eluted fractions were monitored by absorbance at 280 nm and measured for enzyme activities. Alternative elution was performed with 0.1 M GHAG after 1 mg of BLG was applied onto a lactamyl–Sepharose column (0.75 × 4 cm). The peak fractions were pooled and concentrated with a Microcon YM-10 Filter Unit (Millipore, Billerica, MA).

For further purification, the buffer C-eluted fraction from the lactamyl column was applied to ion-exchange high-performance liquid chromatography (HPLC) on a DEAE-5PW column (21.5 × 150 mm, Tosoh Corp., Tokyo, Japan). Elution was performed at a flow rate of 1.0 mL/min at room temperature using two solvents, 10 mM Tris–HCl (pH 7.5) (TBS) containing 1 M NaCl. After injection of the sample, the NaCl concentration was increased linearly from 0 to 0.4 M, and 0.4–1.0 M in 100 min. Each peak was collected and concentrated to measure enzyme activities and subjected to sodium dodecyl sulfate–polyacrylamide gel electrophoresis (SDS–PAGE) and binding studies.

Polyacrylamide gel electrophoresis and zymography

Polyacrylamide gel electrophoresis in the presence of 0.1% SDS was carried out according to the method of Laemmli (1970) under nonreducing conditions using a 9.5 or 7.5% acrylamide separation gel, and native PAGE was performed in the absence of SDS (Davis, 1964). Protein bands were detected with Coomassie Brilliant Blue (CBB) or silver staining (Atto Corp., Tokyo, Japan). For zymography, the gel was incubated in 2.5% Triton X-100 for 1 h after SDS–PAGE to remove SDS or used directly after native-PAGE. The gels were washed and incubated in each substrate solution for several hours at 37°C with gentle shaking. Substrate solutions contained 1 mM X-β-D-glucuronide in 0.2 M sodium acetate buffer (pH 5.0)-50 mM NaCl for BLG.

Solid phase binding assay

Purified BLG fractions eluted from ion-exchange HPLC (each 100 μL) were serially diluted with TBS, placed in the wells of an Immulon I plate (Dynatech Laboratories, Chantilly, VA), and immobilized for 4 h at room temperature. The binding with biotinyl glycoproteins or BP sugar probes (10 μg/mL in TBS) was demonstrated by ELISA using ABC-HRP as described previously (Ueda *et al.*, 1999). Various concentrations of lipids in MeOH (100 μL/well) were dried at 37°C. After the wells were blocked with 3% bovine serum albumin (BSA) in TBS, 100 μL of biotinylated BLG (10 μg/mL) was added to each well, followed by incubation for 2 h. The wells were washed and measured by ELISA as described above.

Measurement of enzyme activity

Enzyme activities were measured in a test tube using a 50 μL aliquot of the sample. For BLG activity, 0.7 mL of 7×10^{-5} M *p*-nitrophenyl-β-D-glucuronide in 0.2 M sodium acetate buffer (pH 5.0)–50 mM NaCl was added to the sample according to the method previously described (Harris *et al.*, 1973). After incubation at 37°C for 1 h, 0.25 mL of 2 M glycine-NaOH (pH 10.4) was added to stop the reaction, and the liberated chromogen, *p*-nitrophenol, was measured at 400 nm. For *N*-acetyl β-galactosaminidase and *N*-acetyl-β-glucosaminidase, *p*-nitrophenyl *N*-acetyl-β-galactosaminide and p-nitrophenyl-*N*-acetyl-β-glucosaminide, respectively, were used as substrates according to the method described previously (Kawai and Anno, 1971). After adding 0.2 mL of 0.7 mM substrate dissolved in 0.1 M sodium acetate buffer (pH 5.0), the test tube was incubated at 37°C for 15 min. Then the reaction was stopped with 1 mL of 0.2 M Na_2CO_3. For β-galactosidase, 0.3 mL of 2 mM *p*-nitrophenyl β-galactoside in 0.05 M sodium citrate buffer (pH 4.0) was added to 30 μL of the sample and incubated at 37°C for 30 min (Li and Li, 1972). The reaction was stopped with 0.9 mL of 0.2 M $Na_2B_4O_7$ (pH 9.8). Arylsulfatase activity was measured under the same conditions as BLG but using potassium *p*-nitrophenylsulfate as a substrate. The concentrations of *p*-nitrophenol were calculated from the absorbance at 400 nm by using free *p*-nitrophenol as a standard ($\varepsilon = 17{,}600\ mol^{-1}$). The specific activity was defined as the amount in μmol of *p*-nitrophenol liberated per minute per mg of protein at 37°C. The protein concentration was determined using a DC Protein Assay Kit (Bio-Rad Laboratories, Hercules, CA) with BSA as the standard.

Kinetic studies were carried out by a microscale assay. The affinity-purified sample (12.5 μL, 10 μg/mL as protein) was added to 175 μL of 0.12 mM to 1.4 mM *p*-nitrophenyl-β-D-glucuronide dissolved in 200 mM sodium acetate buffer–50 mM NaCl (pH 5.0), in the presence or absence of various saccharides (1 μM to 130 mM), in the wells of a plastic microtiter plate at 4°C and mixed well. After incubation for 1 h at 37°C, 62.5 μL of 2 M glycine-NaOH (pH 10.0) was added to each well and mixed, and the absorbance at 405 nm was measured using a microplate reader.

Results

Affinity chromatography of BLG on various carbohydrate-immobilized Sepharose gels

Binding of BLG with various carbohydrate-immobilized gels was studied by affinity chromatography using short columns of various adsorbents, and the activities of the eluted BLG and other enzymes were measured. As shown in Figure 1A, when BLG was bound to an immobilized saccharo-1,4-lactone column, a competitive inhibitor (Kurtin and Schwesinger, 1985), 85% of the activity was eluted with buffer C, and the rest was eluted with buffer D. Surprisingly, *N*-acetyl-β-D-glucosaminidase (β-D-GlcNAcase) and *N*-acetyl β-D-galactosaminidase (β-D-GalNAcase) also bound to and were eluted from the saccharo-1,4-lactone column together with BLG by buffers C and D (Figure 1A). Similar chromatographic behavior of the enzymes was observed on a *p*-aminophenyl β-glucuronide-immobilized column, a substrate for BLG, as shown in Figure 1B, and more than 60% of the activity was eluted with buffer C, together with the other two enzymes. The specific activity and increase in BLG activity and recovery of activities of each enzyme in the fractions eluted from each adsorbent are summarized in Table I. Because of the unexpected chromatographic behavior of

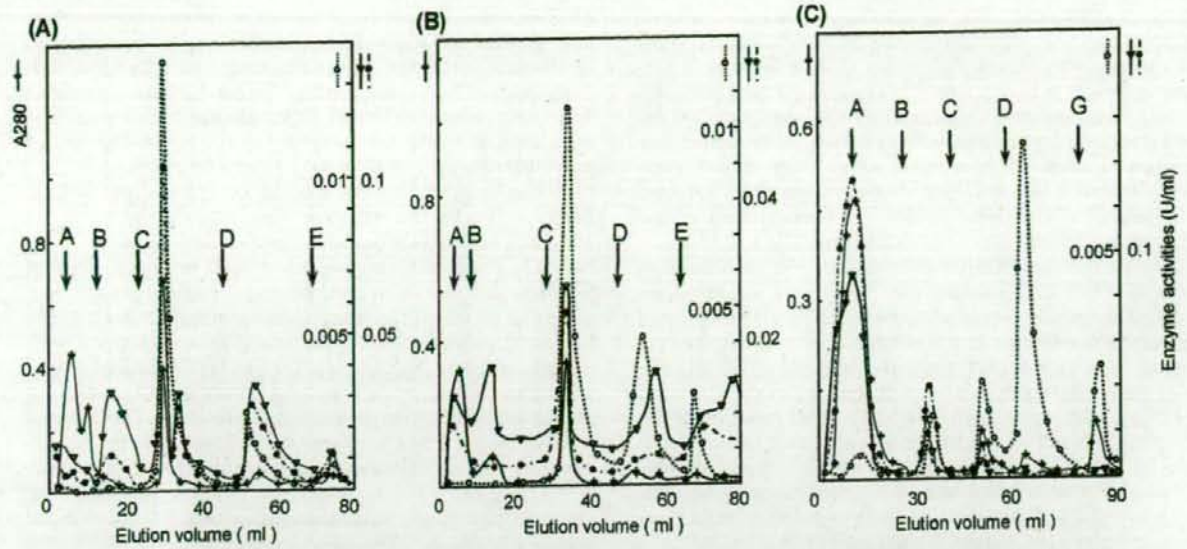

Fig. 1. Affinity chromatography of bovine liver β-glucuronidase (BLG) on a saccharo-1,4-lactone- (**A**), *p*-aminophenyl β-glucuronide- (**B**), and lactamyl- (**C**) Sepharose column. Commercial β-glucuronidase from bovine liver (6 mg from Worthington) was dissolved in buffer A (2 mM sodium acetate buffer [pH 7.0]–5 mM NaCl) and applied to each column (0.75 × 4.5 cm, Vt = 2 ml) at 4°C. The column was washed with buffer A and then sequentially eluted with buffer B (5 mM sodium acetate buffer, [pH 5.0]–5 mM NaCl), buffer C (10 mM sodium acetate buffer [pH 5.0]–5 mM NaCl), buffer D (25 mM sodium acetate buffer [pH 5.0]–5 mM NaCl), buffer E (50 mM sodium acetate buffer [pH 5.0]–5 mM NaCl), buffer G (0.2 M sodium acetate buffer [pH 7.0]–0.2 M NaCl), and 0.1 M sodium borate buffer (pH 7.0). The eluted fractions (2 ml each) were measured at Abs. 280 nm (+), β-D-glucuronidase (○), *N*-acetyl-β-D-glucosaminidase (β-D-GlcNAcase) (●), and *N*-acetyl β-D-galactosaminidase (β-D-GalNAcase) (▼).

the enzymes on these adsorbents, seven other kinds of carbohydrate adsorbents were compared for the ability to separate BLG.

As shown in Figure 1C, lactamyl–Sepharose gave the best separation of BLG from β-D-GlcNAcase and β-D-GalNAcase. BLG bound to the lactamyl–Sepharose column, and 70% of the bound BLG was eluted by the buffer D. In the fractions eluted with buffer D (fraction D), activities of β-D-GlcNAcase and β-D-GalNAcase drastically decreased, and activities of β-D-galactosidase and arylsulfatase were not detected (data not shown). Specific activity of BLG in fraction D increased by 20-fold (Table I). From the other adsorbents summarized in Table I, most BLG activity was eluted by buffer C together with β-D-GlcNAcase and β-D-GalNAcase presenting to various extents. Comparison of the ligand structures of lactamyl– and melibiamyl–Sepharose indicated that β-linked-D-galactopyranosyl residue may contribute to the strong binding and separation of BLG from other enzymes. Based on these observations, the lactamyl–Sepharose column was used for further examination.

Binding characteristics of BLG to lactamyl-Sepharose

The characteristics of BLG binding to lactamyl–Sepharose were studied by microtube assays. As shown in Figure 2A, binding of BLG to lactamyl–Sepharose was maximum at pH 6 and decreased at acidic and basic pH. The amount of bound BLG at pH6 was twice as that at pH 7 in sodium acetate buffer. Based on this result, the binding procedure was hereafter performed at pH 6 (buffer A′) instead of pH 7 (buffer A) to increase the binding capacity.

The abilities of various reagents to elute the bound BLG from lactamyl–Sepharose are summarized in Figure 2B. Buffer G and 5 mM EDTA eluted BLG almost quantitatively, indicating that electrostatic interaction contributes to the binding. Despite the effect of EDTA, addition of Ca^{2+} to the incubation buffer inhibited the binding (data not shown), suggesting that the binding is not Ca^{2+}-dependent and that elution with EDTA may be because of removal of other metal cations or an electrostatic effect. Various sugars including 0.1 M lactose and galactose did not elute more than 20% of the bound BLG from lactamyl–Sepharose (Figure 2B). To examine whether the binding of BLG to lactamyl–Sepharose is a ligand-specific interaction, GHAG, a lactose derivative that is analogous to the ligand structure of lactamyl–Sepharose, was synthesized and studied for ability to elute BLG.

Structural analysis of GHAG and its BLG elution activity

The structure of GHAG was confirmed by NMR. As summarized in Table II, ^{1}H- and ^{13}C-chemical shifts and the coupling constants (data not shown) of the galactosyl residue were in good agreement with typical ones obtained in Me_2SO-d_6 (Iida-Tanaka and Ishizuka, 2000). The chemical shifts of the C-1 carbon in the glucosyl residue, however, did not resonate in the anomeric region, but at 52.7 p.p.m. in the region of the carbon bound by an amino group, -NH-. In addition to the observation of geminal H1 protons, H1a

Table I. Affinity chromatography of β-glucuronidase on various carbohydrate-immobilized Sepharose columns

Adsorbent	Structures of immobilized saccharides	Eluent	Specific activity (mU/mg)	Increase (fold)	Recovery of activity (%) 0 50 100
Saccharo 1,4-lactone-	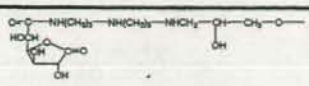	C	78	12	
		D	48	7	
p-Aminophenyl-glucuronide-	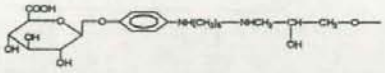	C	82	12	
		D	138	20	
		E	79	11	
Lactamyl-	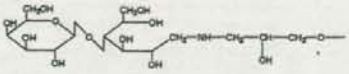	C	19	3	
		D	138	20	
		G	40	6	
Maltamyl-	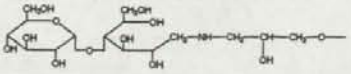	C	80	12	
Melibiamyl-	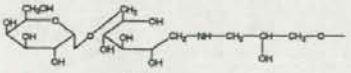	C	93	14	
Glucamyl-	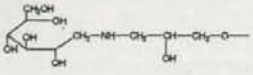	C	58	8	
		D	51	8	
Galactamyl-	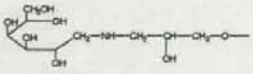	C	45	7	
		D	58	8	
N-Acetylchondrosine-	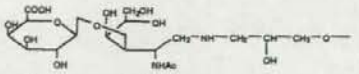	C	114	17	
		D	57	8	
Tri*N*-Acetychitotriamyl-	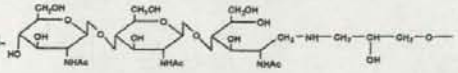	C	44	7	
		F	50	5	

Commercial bovine liver β-glucuronidase (BLG) (6 mg) was dissolved in 1 mL of 2 mM sodium acetate buffer (pH 7.0)-5 mM NaCl (buffer A) and applied to each column (0.75 × 4.5 cm, Vt = 2 ml). The columns were washed with buffer A and then sequentially eluted with 5 mM sodium acetate (pH 5.0)-5 mM NaCl (buffer B) and buffer C–G, as described in the text. The eluted fractions (2 mL/fraction) were measured for enzyme activities and absorbance at 280 nm. The specific activity is expressed as mU/mg, and 1 U produces 1 μmol of the chromogen, *p*-nitrophenol, per minute at 37°C and pH 5.0 under the conditions described in the text. Recovery of activity (%) is expressed by bar, BLG (▬), β-D-GlcNAcase (▪ ▪ ▪), or β-D-GalNAcase activities (· - - - ·).

and b, the above result suggests that the aldehyde group in the glucosyl residue was reductively aminated to produce the structure of -CH_2-NH-. Long-range connectivity of ethanol-C1/Glc-H1s and Glc-C1/ethanol-H1s was observed in the HMBC spectrum.

As shown in Figure 2B, 77% of the BLG activity was eluted from lactamyl–Sepharose with 25 mM GHAG, with small amounts of β-galactosidase and β-GlcNAcase, indicating that most of the BLG bound to lactamyl–Sepharose via the ligand-specific interaction and that GHAG eluted it more effectively than lactose and galactose owing to its structural similarity to the ligand of lactamyl–Sepharose.

Large-scale purification by affinity chromatography on a lactamyl–Sepharose column

The binding of BLG and subsequent washing of the column were performed with buffer A′ at pH 6.0, and BLG was eluted by buffers at pH 5.0. As shown in Figure 3A, all the applied BLG bound to the column at pH 6.0, and a major part of the bound BLG activity was eluted with buffer C (10 mM sodium acetate–5 mM NaCl [pH 5.0]) and buffer E′ (25 mM sodium acetate–25 mM NaCl [pH 5.0]), at slightly lower salt concentrations than those required for elution when the binding was performed at pH 7.0 (cf. Figure 1C).The specific activity of the buffer C-eluted fraction (fraction C) showed a 20 times increase, and the contaminating β-galactosidase and β-D-GalNAcase markedly decreased. Increasing the ion concentration to 200 mM sodium acetate buffer–200 mM NaCl (pH5.0) (buffer G) did not elute any proteins (data not shown). As shown in Figure 3B, GHAG eluted BLG as a single peak from a lactamyl–Sepharose affinity chromatography column.

The buffer C- and GHAG-eluted fractions showed similar protein patterns on SDS–PAGE (Figure 3C). Zymography of both the fractions indicated the presence of an active

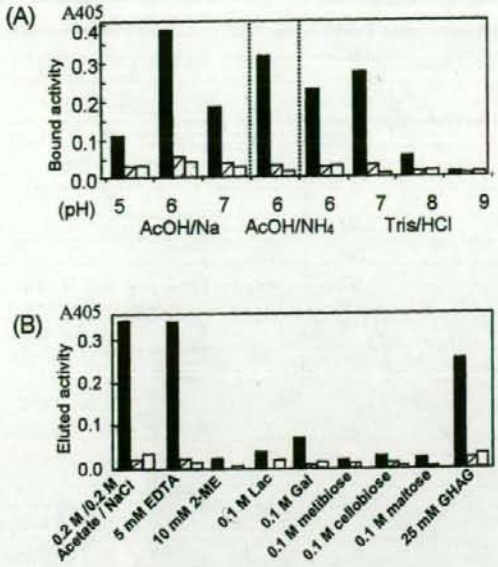

Fig. 2. Optimum binding and elution condition of bovine liver β-glucuronidase (BLG) to lactamyl–Sepharose. (**A**) Lactamyl–Sepharose 4B (0.1 g) and BLG dissolved in 0.3 ml of various buffers (3.3 mg/ml): 2mM sodium acetate buffer (pH 5–6), ammonium acetate buffer (pH 6), or Tris–HCl (pH 6–9), each containing 5 mM NaCl, were incubated in 1.5 ml tube at 4°C for 4 h. After centrifugation, the supernatant was removed, the gel was washed three times with the same buffer, then the bound BLG was eluted with buffer G (0.2 M sodium acetate buffer [pH 5.0]–0.2 M NaCl) for 4 h at 4°C, and measured for its enzyme activity. (**B**) To study the elution from lactamyl–Sepharose gel 0.2 ml of BLG solution in buffer A′ (2 mM sodium acetate buffer [pH 6.0]–5 mM NaCl) at 5 mg/mL concentration was incubated with 0.1 g of lactamyl–Sepharose gel. After centrifugation, the supernatant was removed, the gel was washed three times with the same buffer, and then the bound proteins were eluted with incubation in 0.2 mL of each elution buffer or eluate in buffer A′ for 4 h at 4°C. The enzyme activities of washed and eluted fractions were measured separately.

Table II. ^{1}H- and ^{13}C-chemical shifts (p.p.m.) of 1-deoxy-4-*O*-β-D-galactopyranosyl-1-[(2-hydroxyethyl)amino]-D-glucitol (GHAG)

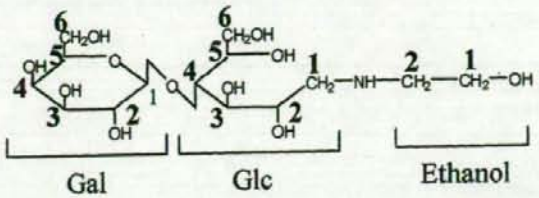

Residue	^{1}H-chemical shift (p.p.m.)		^{13}C-chemical shift (p.p.m.)	
Ethanol	H1a	3.45	C1	60.1
	H1b	3.48	C2	52.0
	H2a	2.57		
	H2b	2.57		
Glc	H1a	2.40	C1	52.7
	H1b	2.69	C2	69.6
	H2	3.84	C3	71.1
	H3	3.52	C4	81.3
	H4	3.52	C5	71.1
	H5	3.67	C6	62.5
	H6a	3.56		
	H6b	3.59		
Gal	H1	4.21	C1	104.4
	H2	3.30	C2	71.2
	H3	3.26	C3	73.5
	H4	3.59	C4	68.9
	H5	3.33	C5	75.9
	H6a	3.46	C6	61.5
	H6b	3.54		

^{1}H- and ^{13}C-signals were assigned based on the double quantum-filtered correlated spectroscopy (DQF-COSY), total correlated spectroscopy (TOCSY), and heteronuclear multiple-quantum coherence (HMQC) spectra, and the relationships between the residues were confirmed by heteronuclear multiple-bond correlation (HMBC) experiment.

form of BLG at the migration position corresponding to 160 kDa, whereas the 78-kDa subunit monomer was shown to be inactive (Figure 3C, lanes e–f). The reported molecular size of the active BLG in solution, 290 kDa, on sucrose density gradient centrifugation was considered to be a tetramer of the 78-kDa subunit (Himeno *et al.*, 1974). The reason for the discrepancy between the reported and observed molecular mass is yet unclear, but the possibility that the 160-kDa band on SDS–PAGE is a tetramer cannot be denied. Another possibility is that the 160-kDa band corresponded to a dimer whose activity was recovered after removing SDS. In this case, whether active BLG forms a tetramer in gel or remains a dimer is unknown. As shown in Figure 3C, the buffer C eluted fraction more of the active form of BLG than of the monomer, whereas the monomer is predominant in the GHAG-eluted fraction. The BLG activity in fraction E′ in Figure 3A was lost after PAGE (data not shown) possibly because a factor that stabilizes the active form may have been removed in fraction E′ and the activity could not be restored after PAGE. Based on these observations, fraction C was subjected to further purification because it still contained a few other protein bands. BLG purchased from Sigma gave essentially the same elution profile on lactamyl–Sepharose column and protein bands on SDS–PAGE as those of BLG obtained from Worthington (data not shown).

Ion exchange HPLC of BLG on DEAE-5PW

Fraction C was separated into five fractions by NaCl gradient on ion-exchange HPLC on a DEAE-5PW column, as shown in Figure 4A. Peak b exhibited β-glucuronidase activity with trace activity of other enzymes (Figure 4B), and a single protein band corresponding to the monomeric BLG on SDS–PAGE under reducing conditions (Figure 4C). β-Galactosidase activity was detected mainly in peak c. In the course of the study, gel filtration HPLC was also tried for further purification of fraction C. In that case, β-galactosidase was separated from the

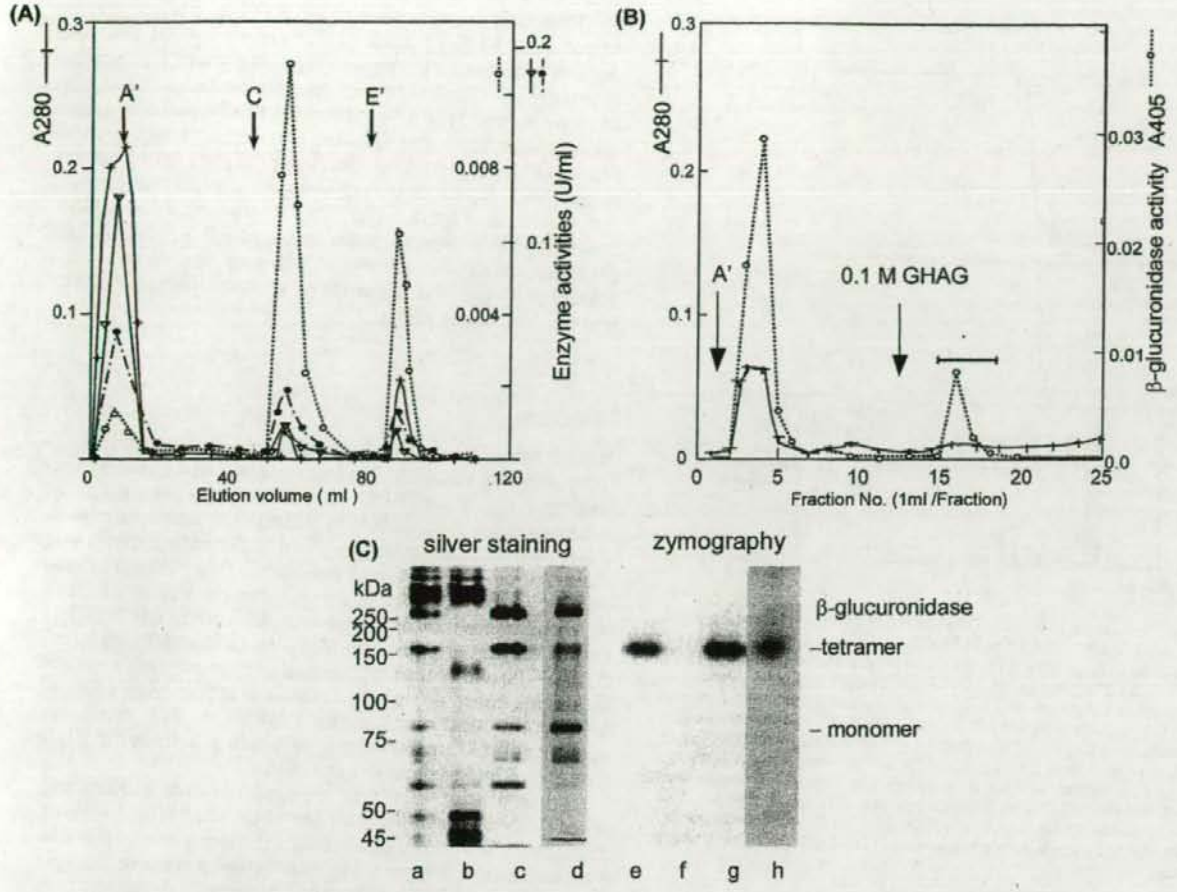

Fig. 3. Affinity chromatography of bovine liver β-glucuronidase (BLG) on a lactamyl–Sepharose column. (**A**) BLG (Worthington, 15 mg) was mixed with 13 ml of lactamyl–Sepharose 4B in buffer A′ and incubated for 5 h at 4°C with gentle shaking; then the gel was poured into a column (1.5 × 8 cm) and washed with buffer A′. BLG was successively eluted with buffer C and buffer E′. (**B**) BLG (sigma, 1mg) in buffer A′ was applied onto a lactamyl column (0.75 × 4 cm) and washed with buffer A′. BLG was eluted with 0.1 M 1-deoxy-4-*o*-β-D-galactopyranosyl-1-[(2-hydroxyethyl)amino]-D-glucitol (GHAG). Eluted fractions were monitored at 280 nm and by enzyme activity. (**C**) Sodium dodecyl sulfate–polyacrylamide gel electrophoresis (SDS–PAGE) patterns of fractions eluted from the lactamyl–Sepharose column. Silver staining (lanes a–d) and zymography for detecting BLG activity (lanes e–h). Lanes a and e, crude BLG; lanes b and f, the washed fraction (fraction A′); lanes c and g, fraction C; lanes d and h, the 0.1 M GHAG-eluted fraction.

BLG peak, but β-glucosaminidase and β-galactosaminidase activities remained in the BLG peak (data not shown).

Effect of free saccharides on BLG activity

BLG activity was measured using fraction C from lactamyl affinity chromatography as BLG in the presence or absence of various saccharides (1 μM to 130 mM) at 0.12 mM to 1.4 mM substrate concentrations. The results are summarized in Table III, and examples of the double reciprocal of Lineweaver–Burk plots are shown in Figure 5. According to the Lineweaver–Burk plot analyses, BLG is dependent on the lactose concentration, as shown in Figure 5A. At 1 mM lactose, the interception of the *x*-axis (1/Km) of the plot was unchanged from that of the control, indicating that lactose binds to both the free enzyme and the enzyme–substrate complex. The result suggests that the lactose-binding site of BLG is different from the catalytic site. On the contrary, at lactose concentrations higher than 13 mM, the plot showed a tendency toward competitive inhibition with the interception with the *y*-axis (1/Vmax) unchanged. In contrast, saccharo-1,4-lactone (1 μM) and D-glucuronic acid (1 mM) showed a typical competitive inhibition, as shown in Figure 5B. Cellobiose showed a very weak tendency toward non-competitive activation. On the contrary, other tested saccharides, maltose (Figure 5C), D-glucose and D-galactose mannose-6-phosphate, *N*-acetylglucosamine, and *N*-acetylneuraminic acid (1 mM), did not have a significant or integrative effect on the enzyme activity, although BLG bound to the affinity adsorbents of some of these saccharides.

Binding studies of BLG with glycoproteins and lipids

The binding activities of purified BLG to biotinyl glycoprobes were studied at pH 7.5 and pH 5.0 by solid-phase binding assay. At pH 5, BLG did not bind to any of tested